ISAS - INTERNATIONAL SCHOOL
FOR ADVANCED STUDIES

STRUCTURAL STUDIES OF NISIN BY MEANS OF 2D-NMR

Thesis Submitted for the Degree of
Magister Philosophiae

Candidate: Federico Fogolari

Supervisors: Dr. Frank J. M. Van de Ven

Prof. Antonio Borsellino

Academic Year 1989/90

TRIESTE

SISSA - SCUOLA
INTERNAZIONALE
SUPERIORE
DI STUDI AVANZATI
TRIESTE
Strada Costiera 11

STRUCTURAL STUDIES OF NISIN

BY MEANS OF 2D-NMR

Thesis Submitted for the Degree of
Magister Philosophiae

Candidate: Federico Fogolari

Supervisors: Dr. Frank J. M. Van de Ven

Prof. Antonio Borsellino

Academic Year 1989/90

Contents

Introduction 1
Nisin 2
Theory 7
Basic facts about N.M.R. 7
2D FT experiments 10
Double quantum filtered COSY 11
NOESY 14
TOCSY 15
Experimental 19
The assignment of the 1H spectrum 19
Results and discussion 35
Nisin spectrum in water and water/TFE mixture . . . 35
Noesy spectra and distance constraints 36
Nisin structure from distance constraints 39
Conclusions 44
References 46
Acknowledgements 48

Introduction

Membrane proteins carry out many important cell functions like the communication with the environment and with other cells. The list of functions these membrane components perform includes active transportation of ions or small metabolites, selective permeabilization of the membrane, energy transduction, recognition of neurotransmitter and hormones and also control of some viral infection. Notwithstanding their biological interest the knowledge about this class of proteins is not even comparable to that available for soluble proteins, at least at a molecular level. The reason for this may be traced back to the difficulties in obtaining 3D crystals and as a consequence the impossibility of resolving their spatial structure by means of x-ray cristallography.

Most of these proteins (e.g. ionic channels) are too large to study their 3D structure by means of high resolution N.M.R. and for smaller ones getting a suitable sample is still a difficult task. To render these considerations more effective we can report a figure: up to 1988 no more than 20 membrane proteins had been crystallized (Kuhlbrandt 1988) and certainly for much less the 3D structure had been obtained by means of N.M.R..

The knowledge on the principles of protein–lipid interaction is, for the reasons mentioned above, still not very detailed. All the data available point to hydrophylic and hydrophobic interactions as the driving forces, but no more detailed general model has been proposed yet.

The application of N.M.R. to this problem is important also for another reason: membrane proteins are designed to work in an amphiphylic (that is a very specific) environment and therefore the experimental conditions are expected to determine the outcome of any investigation. Obviously a crystal is not expected to be representative of *in vivo* conditions, however the confirmation of the reliability of X–ray cristallography for soluble proteins came from comparison with the analogous solution N.M.R. studies. A similar check for membrane proteins would give more confidence to the results obtained by means of X–ray cristallography.

Apolar solvents and detergent micelles are being used to mimic lipid bilayer membranes. Solubility and control over the micelle dimensions constitute still the

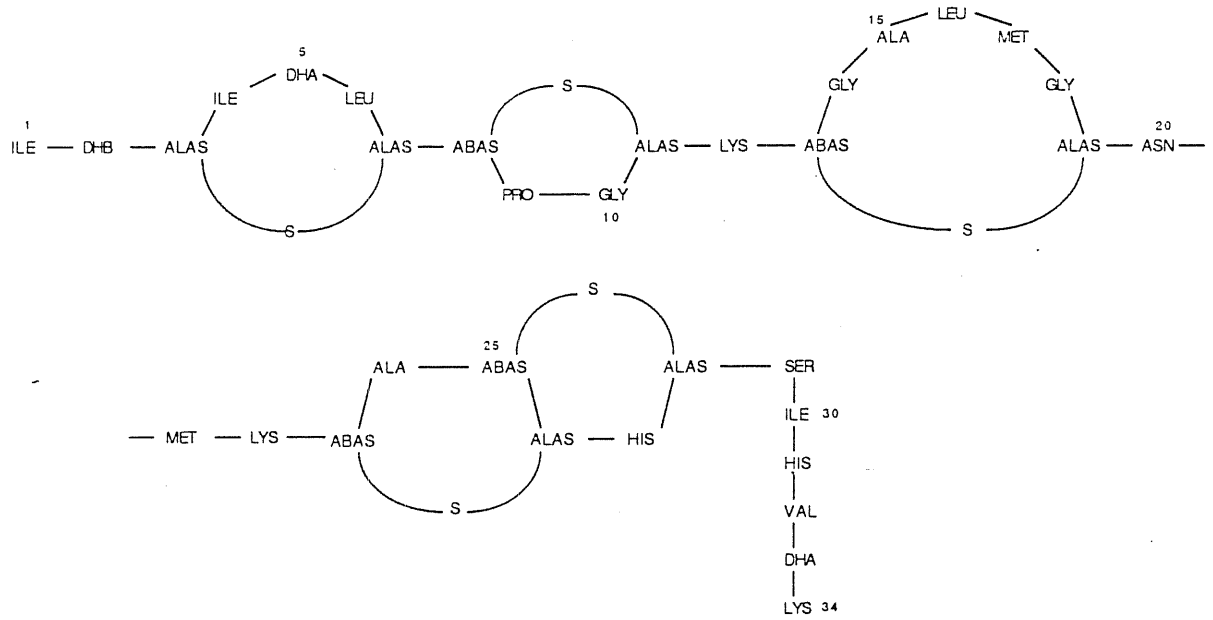

Fig. 1 The primary sequence of Nisin. Standard abbreviations for the amino acids are used. Alas, Abas, Dha and Dhb residues are described in the text.

main difficulty.

A research program was started involving the study of Nisin (fig. 1) (a small polypeptide) in aqueous and apolar solvent and possibly in detergent micelles. We hope to gain insight on the principles of the protein insertion in the membrane comparing the results obtained in the experiments performed in different solution conditions. We hope also that knowledge of the 3D structure will unravel its structure-function relationship.

NISIN

Nisin (from N inhibitory Substance) is a polypeptide produced by certain strains of Streptococcus lactis belonging to Lancefield serological group N, containing unusual amino acids such as Lanthionine (Lan), Methyl–lanthionine (MeLan) (Knox & Keck 1973,1975) , Dehydro–alanine (Dha) and Dehydro–butyrine (Dhb)

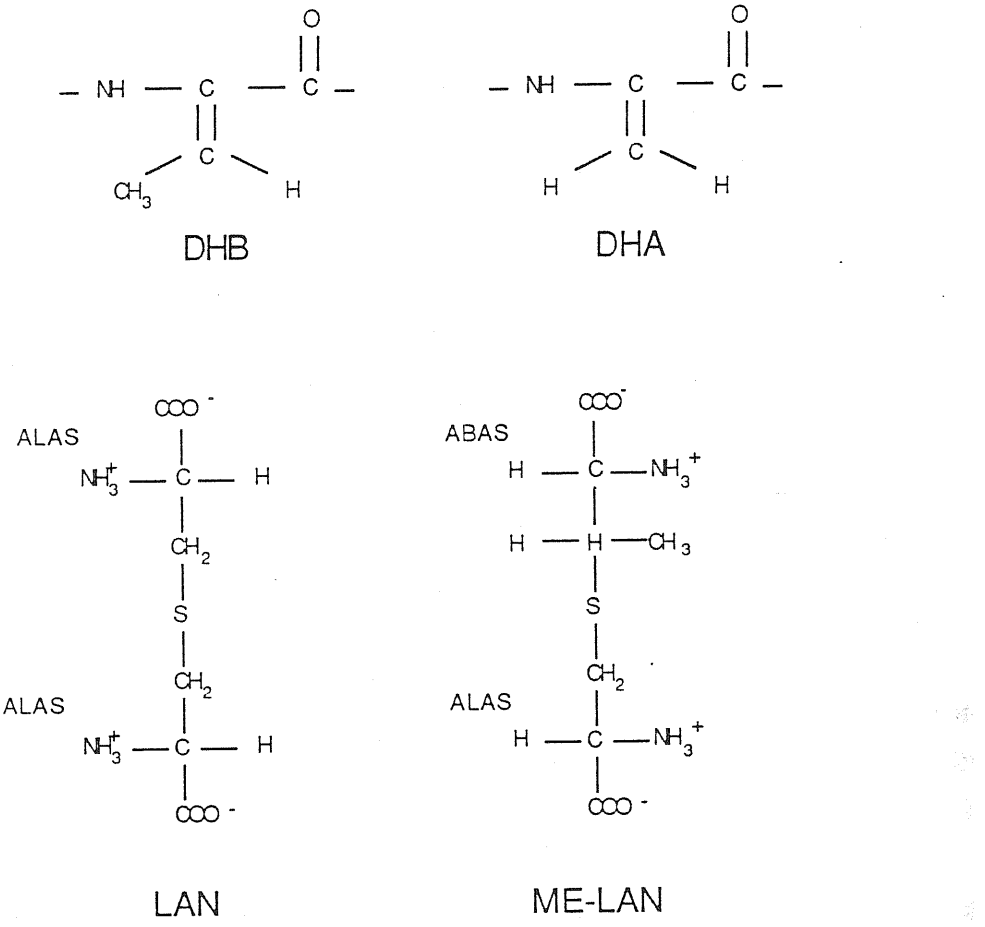

Fig. 2 The unusual amino acids of Nisin: Dha = Dehydroalanine, Dhb = Dehydrobutyrine, Lan = Lanthionine, MeLan = Methyl–Lanthionine (Lateral atoms and groups in Lan and MeLan are pointing outside of the paper plane). The moieties of the latter two will be indicated in the following as Alas and Abas (from Alanine and Aminobutyric acid). The existence of two chirally symmetrical Alas must however be kept in mind.

(fig.2).

It shares this peculiar feature with a whole class of antibiotics which have been termed Lantibiotics (Schnell et al. 1988) and which include also Epidermin, Subtilin, Cinnamycin, Duramycin, Ancovenin, Ro09–0198 and Pep5. It exhibits antimicrobial activity against Gram–positive bacteria and inhibits sporulation of Bacilli and Clostridia. For this reason and for its non–toxicity it is used as a food

preservative (being a polypeptide any residue of it, still present in the food, is easily digested). Further advantages concerning its use could be a reduction in heat treatment, with consequent benefits, due to its capability to render spores more heat sensitive (Hurst 1981).

Although Nisin has been known for quite a long time, its primary structure was published only in 1971 (Gross & Morell 1971) and its biosynthesis, functions and mode of action are being understood in these years. It was shown in 1988 for Epidermin (Schnell et al. 1988) and in 1989 for Nisin (Kaletta & Entian 1989) that these Lantibiotics are the result of post–translational processing of ribosomally synthesized pre–peptides. The sequences of the two genes showed a high degree of analogy strongly suggesting a common pathway to the synthesis of the mature molecules involving several steps as water elimination, double bond formation, sulphide ring formation and cleavage (fig.3).

In particular both the precursors include the corresponding polypeptide as the C–terminal while the N–terminals show a very high degree of structural analogy indicating their essential role in the molecules biosynthesis. The confirmation of the extendability of these findings to the whole class of the Lantibiotics is, possibly, to come in the very near future.

As to the functions of Nisin a role as a dominance factor seems well established (the most sensitive organism to it is Streptococcus Cremoris which is competing for the same ecological niche) while there is experimental evidence that Nisin is involved, possibly as a regulator, in the growth of the cell (for a review see Hurst 1981).

Research on the mode of action of Nisin has been going on for at least four decades now but full understanding hasn't been reached yet. Interaction with the cytoplasmic membrane and inhibition of Murein synthesis has been clearly demostrated by several authors. The latter doesn't seem to be the main mechanism of action for several reasons: long times and high concentration are required and activity against organisms lacking this polymer was also found (Reisinger et al. 1980, Henning et al. 1986). Recently a voltage dependent interaction with phospholipid membranes has been demonstrated. Addition of Nisin to energized cells cause a rapid efflux of low molecular weight substances and an immediate drop of the membrane potential (Ruhr & Sahl 1985, Kordel & Sahl 1986). Experiments

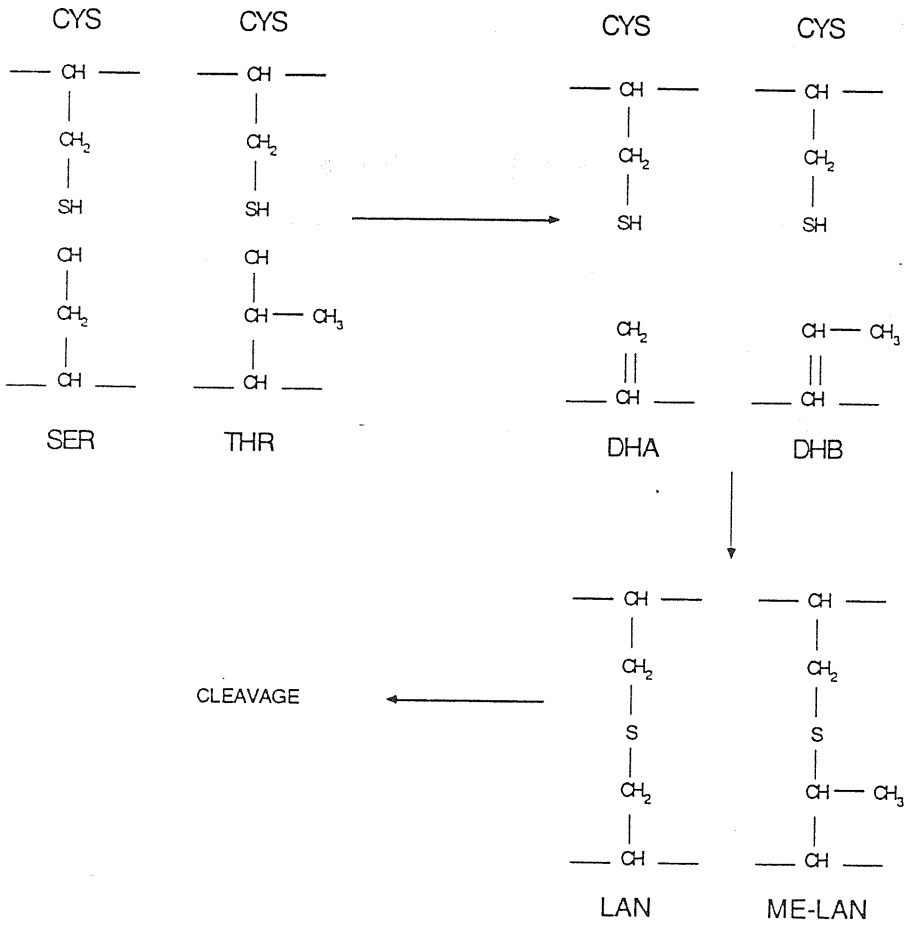

fig. 3 Possible steps, based on the scheme proposed by Ingram (Ingram 1970) in Lantibiotics biosynthesis: 1) a precursor is synthezised containing Threonines, Cysteines and Serines, 2) Serines and threonines are dehydrated to Dehydroalanines and Dehydrobutyrines, 3) Addition of Cysteines to dehydroresidues proceeds via thio–ether bridge formation with stereo–inversion.(After Buchman et al. 1988).

were also performed on black lipid bilayer membranes and macroscopic and single channel currents were recorded. Nisin forms multistate pores whose conductances and related fluctuations vary from membrane to membrane and with the potential applied (the largest single channel conductance is consistent with a pore diameter of 0.9 nm). The threshold potential for Nisin action found for artificial membranes (-100 mV with Nisin added on the zero potential side) is much higher, in absolute value, than that found for natural membranes and this could be due to the interaction of Nisin with some integral components of the membrane (Sahl et al. 1987,

Morris et al. 1984) facilitating the peptide insertion in the membrane. However since Nisin is expected to bear a positive charge in the range of its solubility conditions (Hurst 1981) the significance of the requirement of a potential difference through the membrane is not fully understood. This voltage difference could be needed to control the protein insertion in the membrane or simply to create, via a Poisson–Boltzmann distribution, a higher concentration at the cytoplasmic surface or also to force the already formed pore in a conducting state.

Theory

BASIC FACTS ABOUT NMR

N.M.R. is a phenomenon associated with nuclei possessing angular momentum and magnetic moment. (A comprehensive review on the physical principles of N.M.R. can be found in the book of Abragam (1961), for more recent developments an excellent text has been published by Ernst & al. (1989) and a very good book dealing with N.M.R. of proteins and nucleic acids is the one by Wüthrich (1986))

a) Classical treatment – Consider a system with angular momentum $\vec{L} = \hbar\vec{I}$ (where $\hbar$ is as usual the planck's constant divided by 2π and $\vec{I}$ is an a–dimensional vector assuming integer or semi–integer values) and associated magnetic moment $\vec{M} = \gamma\vec{L}$, (where γ is the gyromagnetic ratio) the classical equation for this system is

$$\frac{d\vec{L}}{dt} = \gamma\vec{L} \times \vec{H}$$

and if we turn to a reference frame rotating with frequency $-\omega$ (the minus sign means left–hand rotation) around axis $\vec{k}$, then the same equation holds with $\vec{H}$ replaced by $\vec{H}_{eff} = (\vec{H}_{rot} - \frac{\omega}{\gamma}\vec{k})$, where $\vec{H}_{rot}$ is the magnetic field expressed in the rotating frame coordinates. Two cases are interesting:

1) $\vec{H} = \vec{H}_0\vec{k}$ (static field) $\vec{M}$ precesses in the laboratory frame with (resonance) frequency $-\omega_0 = -\gamma\vec{H}_0$ around $\vec{k}$

2) $\vec{H} = H_0\vec{k} - H_1(\vec{i}\cos\omega_0 t - \vec{j}\sin\omega_0 t)$ where $\omega_0 = \gamma H_0$. In the frame rotating at the resonance frequency along $\vec{k}$ only a static field $-H_1\vec{i'}$ is left and the magnetization precesses around $\vec{i'}$ with frequency $\omega_1 = \gamma H_1$. If the rotating field is applied for a time t_p the angle $\omega_1 t_p$ is called the flip angle of the pulse.

b) Quantum mechanical treatment – In the Heisenberg representation we have

$$\frac{\hbar}{i}\frac{d\vec{I}}{dt} = [\mathbf{H}, \vec{I}] = [\gamma\hbar\vec{H}\cdot\vec{I}, \vec{I}] = \gamma\hbar\vec{I} \times \vec{H}$$

so the expectation value for $\vec{I}$ follows the classical equation. If we have a statistical ensemble of spins we must turn to a density matrix treatment (Fano 1957). If every

system can be described by a wave function $|\psi\rangle = \sum_m a_m|\psi_m\rangle$ we call density operator the operator having the following matrix elements:

$$\sigma_{mm\prime} = \langle\psi_m|\sigma|\psi_{m\prime}\rangle = \overline{a_m a_{m\prime}}$$

where the bar indicate the ensemble average. If we chose an orthonormal basis O_i (i.e. $Tr(O_iO_j) = \delta_{ij}$) then the coefficients c_i of the density operator expansion in this basis will be simply the expectation value of the corresponding basis operator:

$$< O_k >= Tr(O_k\sigma) = Tr(\sum_i O_k c_i O_i) = \sum_i c_i\delta_{ik} = c_k$$

Therefore it is useful to have among the basis operators also the observables or the "coherences" we are interested in. Every non zero off–diagonal element of the density matrix reflects a coherence in the phases of the coefficients of the single system wave function expansion. It is worthwhile at this point to introduce the concept of "phase cycling" (Bain 1984, Bodenhausen & al. 1984) . In general we can expand the density matrix in components corresponding to p–quantum coherences:

$$\sigma = \sum_p \sigma^p$$

(we call p–quantum coherences the coherent superposition of states differing in their m_z quantum number by $\Delta m_z = \pm p$). Suppose we have a unitary transformation U (it can be brought about by a sequence of pulses) such that : $\sigma^{p\prime} = U\sigma^p U^{-1}$ If we change the phase of U obtaining $U' = exp(-i\sum_i I_{iz}\phi)Uexp(i\sum_i I_{iz}\phi)$ (this amounts to rotating the space around $\vec{k}$ by an angle ϕ) we get $U'\sigma^p U'^{-1} = \sigma^{p\prime}exp[i(p - p\prime)\phi]$. By summing the signals from experiments performed with different pulse phases we can get rid of the unwanted coherences. Since we can expand the density matrix in p–quantum coherence terms at every step of the experiment we can also follow the coherence pathway of every term of the final density matrix (keeping in mind that only single coherences like I_x or I_y can be measured). The process of changing the phase of the pulse sequence (or of part of it) and summing the relative signals is referred to as "phase cycling".

Useful further effects derive from:

a) the direct interaction with the electrons surrounding the nucleus – In the presence of an applied field the Larmor precession of the induced orbital magnetic

moment of the electrons creates a diamagnetic field at the nucleus while the distorsion of the electrons wave function produces a second field opposite in sign to the previous one. Since both are proportional to the primary field applied H_0, the effective field will be $H_0(1-\sigma)$. σ is called the chemical shift. Although its explicit calculation is not straightforward we can assign regions of the spectrum to specific types of atoms (for instance amide protons have always chemical shifts different from methyl protons)

b) the indirect interactions among the nuclei mediated by the electrons – If we consider the second order terms in the perturbative expansion of the Hamiltonian of the nuclei and the electrons of one molecule, assuming isotropic molecular tumbling, we get an Hamiltonian of the following type

$$\mathrm{H}_{12} = J_{12}\vec{I}_1 \cdot \vec{I}_2$$

where J_{12} could be in principle calculated, but this would require the knowledge of all the excited states of the molecule. The coupling constant J_{12} can be, in some cases, empirically connected to the dihedral angles involving the coupled atoms through so–called "Karplus–type" relations (for biological applications see Wütrich 1986 and Altona 1982).

c) the direct through space dipolar coupling with other nuclei and with the lattice – As a consequence of the random character of this kind of interactions all the effects can be taken into account by means of a relaxation matrix for the expectation values of the magnetization (Solomon 1955). We can get expressions for T_1 and T_2 (respectively the longitudinal and trasversal relaxation rates) and for the cross–relaxation rates assuming isotropic tumbling, no mechanisms of relaxation other than dipolar coupling and unlike spins. The time evolution of the magnetization M_z toward its equilibrium value M_z^0 can be described by the following equations:

$$\frac{d\vec{M}_z}{dt} = -R\vec{M}_z$$

where

$$\vec{M}_z = \begin{pmatrix} M_{1z} - M_{1z}^0 \\ M_{2z} - M_{2z}^0 \\ \vdots \\ M_{nz} - M_{nz}^0 \end{pmatrix}$$

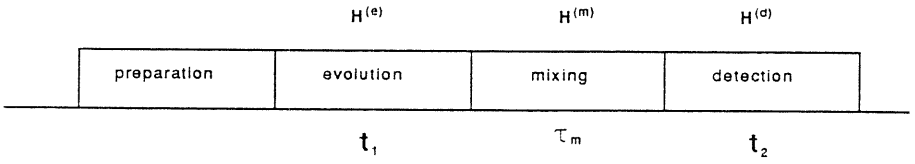

fig. 4 Basic scheme for a 2D FT N.M.R. experiments: $\mathbf{H}$ indicates the Hamiltonian governing the time evolution

and the coefficients of R (the relaxation matrix) are:

$$R_{ii} = \sum_{j \neq i} q_{ij}(J(\omega_i - \omega_j) + 3J(\omega_i) + 6J(\omega_i + \omega_j))$$

$$R_{ij} = q_{ij}(J(\omega_i - \omega_j) - 6J(\omega_i + \omega_j))$$

with $q_{ij} = \frac{\gamma_i^2 \gamma_j^2 \hbar^2}{10}$. In the assumption of a single exponential correlation function the spectral density is a very simple function of the rotational correlation time τ_c:

$$J(\omega) = \frac{\tau_c}{1 + \omega^2 \tau_c^2}$$

Additional relaxation rates to be included in the above formulae are due to interaction with the lattice and can be computed as a function of the intensity and decay constant τ_0 of the random fluctuating field experienced by expressions:

$$\frac{1}{T_1} = 2\gamma^2 \overline{H}_{tr}^2 \left(\frac{\tau_0}{1 + \omega_0^2 \tau_0^2}\right) \qquad \text{for longitudinal magnetization}$$

and

$$\frac{1}{T_2} = \gamma^2 \left(\overline{H}_{long}^2 + \overline{H}_{tr}^2 \frac{\tau_0}{1 + \omega_0^2 \tau_0^2}\right) \qquad \text{for transversal magnetization.}$$

2D FT EXPERIMENTS

A two–dimensional (2D) Fourier Transform (FT) experiment is basically the straightforward extension of the common 1D experiments. Whereas a function of the time domain $s(t)$ is transformed to give a spectrum in the frequency domain, in the 2D experiments a signal depending on two time intervals $s(t_1, t_2)$ is converted in a 2D frequency spectrum. The basic scheme of a 2D–experiment is given in fig. 4.

We can divide an ideal 2D N.M.R. experiment in four periods of time. Although these can be of different nature and also overlapping we can understand the principles of the experiment following this scheme.

1) The preparation period is devoted to create a coherent non–equilibrium state of the spin system (for instance a non selective $\frac{\pi}{2}$ pulse could suffice to this purpose).

2) During the evolution period the system evolves under the Hamiltonian $\mathbf{H}^e$ (in the simplest case this could be the free precession Hamiltonian). The duration of this period t_1 is incremented from an experiment to another, so that memory of the evolution will be kept in the ω_1 frequencies.

3) The mixing period is designed to let the system evolve under the Hamiltonian bearing the information we want to get from the experiment (for instance a TOCSY Hamiltonian giving information on J–coupling).

4) During the detection period the system evolves under the Hamiltonian $\mathbf{H}^d$ (for instance again the free precession Hamiltonian) and the transverse magnetization is recorded as a function of t_2.

After 2D Fourier Transform a 2D frequency spectrum is obtained. This scheme will become clearer in the following illustration of the three kind of experiments actually performed in the study of Nisin.

DOUBLE QUANTUM FILTERED COSY

To describe the Double quantum filtered (DQF–) COSY experiment (fig. 8) it is useful to introduce the following basis for the Liouville space: the basis operators are obtained taking the product of the single spin operators E_i, I_{ix}, I_{iy} and I_{iz} (for spin i). This choice is easily understood if we consider that cyclic commutation rules hold among these basis operators for $I = \frac{1}{2}$ spins, so that if $[O_k, O_l] = \pm iO_m$ than $[O_m, O_k] = \pm iO_l$. Using this basis we can easily treat the evolution of the system under an Hamiltonian proportional to one of the basis operators. in fact we have

$$exp(i\theta O_p)O_q exp(-i\theta O_p) = \begin{cases} O_q & \text{if } [O_p, O_q] = 0; \\ O_q cos\theta + i[O_p, O_q] sin\theta & \text{if } [O_p, O_q] \neq 0 \end{cases}$$

so that the evolution of the system under such an Hamiltonian can be represented by a very simple diagram (fig. 5)(Van de Ven & Hilbers 1983).

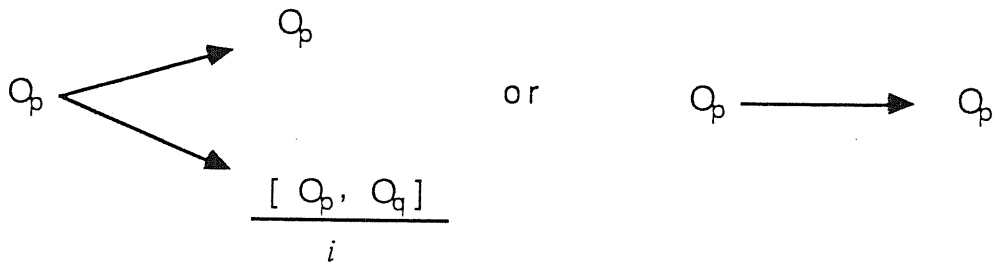

Fig. 5 Diagramatic representation of the operator evolution when cyclic commutation rules apply between the operators O_i. The upper branch is the cosine term while the lower branch is the sine term or, alternatively, the operator is left unchanged by the evolution operator.

This formalism can readily be applied to all those experiments where infinitely strong and sharp pulses are assumed and there is only weak coupling among the spins (this is usually the case if the main field term is still present in the Hamiltonian). Before describing the DQF–COSY experiment we give a summary of a standard COSY experiment (Aue et al. (1975)).

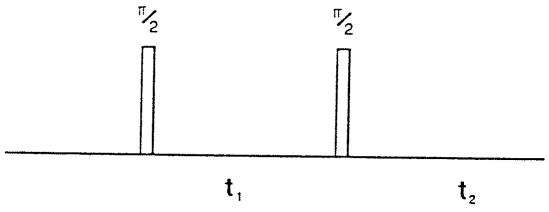

Fig. 6 Basic scheme of the COSY experiment

The basic scheme and the evolution diagram are reported in fig. 6 and 7. If we collect the observable single coherence terms we have the following time signal:

$$
\begin{aligned}
-M_y(t_1,t_2) &= -\gamma\hbar(< I_{1y} > + < I_{2y} >) = \\
&= \frac{1}{4}\gamma\hbar[(\cos(\omega_1 - \frac{1}{2}J_{12})t_1 - \cos(\omega_1 + \frac{1}{2}J_{12})t_1)\cdot \\
&(\cos(\omega_2 - \frac{1}{2}J_{12})t_2 - \cos(\omega_2 - \frac{1}{2}J_{12})t_2) + \\
&(\sin(\omega_1 + \frac{1}{2}J_{12})t_1 + \sin(\omega_1 - \frac{1}{2}J_{12})t_1)\cdot \\
&(\sin(\omega_1 + \frac{1}{2}J_{12})t_2 + \sin(\omega_1 - \frac{1}{2}J_{12})t_2)]
\end{aligned}
$$

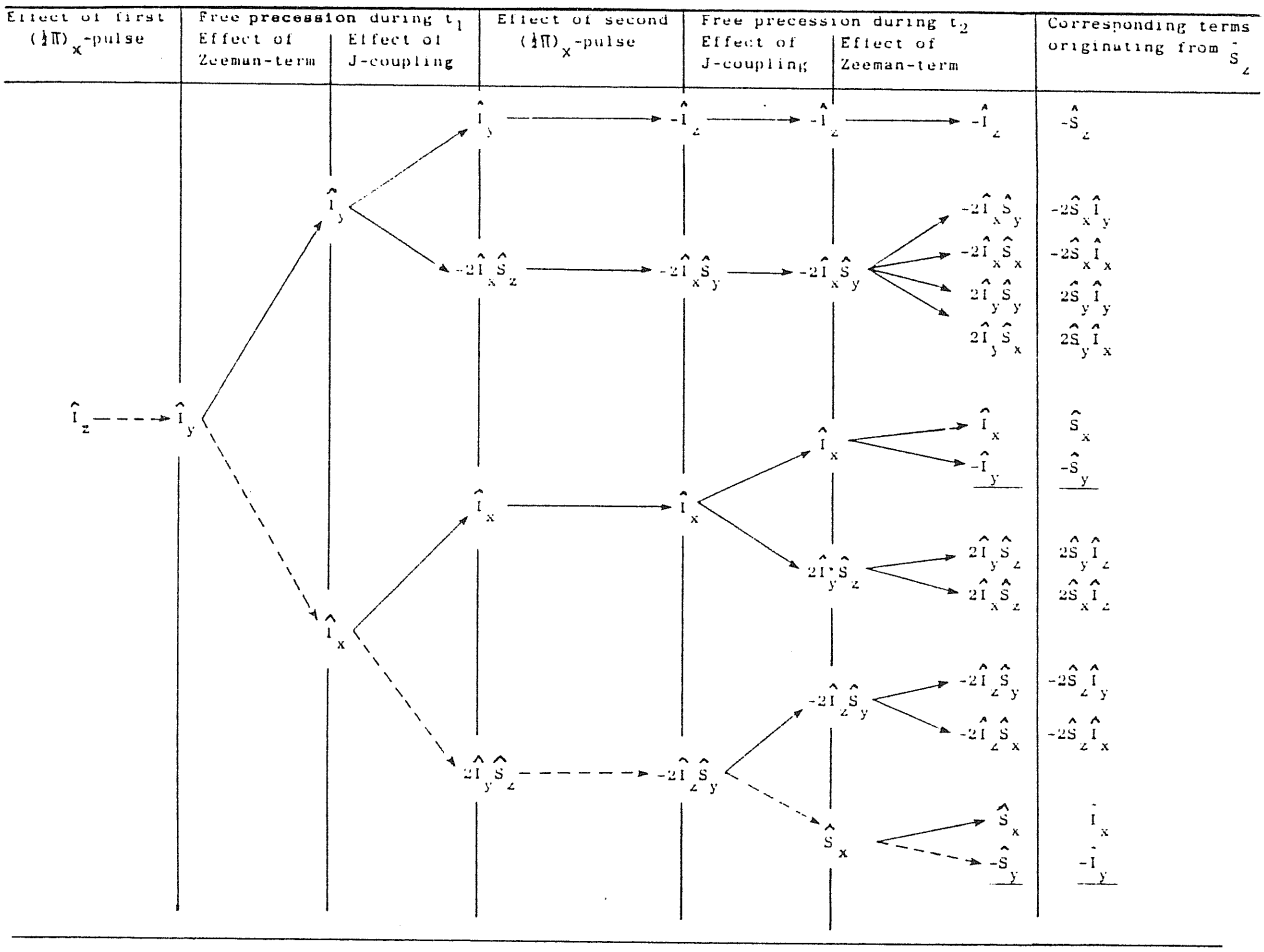

Fig. 7 Evolution diagram of the magnetization for a two–spin system $\vec{I}$ and $\vec{S}$ during the COSY experiment. (After Van de Ven & Hilbers 1983).

that, after 2D FT gives a 2D spectrum where the crosspeaks connect the resonance positions of J–coupled spins.

An unwanted feature of this spectrum is that if the phase is chosen in order to have the diagonal peaks in pure 2D absorption mode the crosspeaks will be in pure 2D dispersion mode.

To overcome this difficulty DQF–COSY was proposed (Rance et al. 1983); a third pulse is inserted immediately after the second one so that double quantum coherences at the end of the second pulse are converted into single quantum coherences that are observed during t_2 . All the other coherence pathways are rejected by the appropriate phase cycling. The spectrum obtained in this way can be phased in order to have both diagonal and crosspeaks in a pure 2D absorption mode with

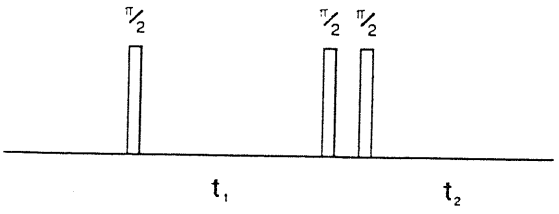

Fig. 8 Basic scheme of the DQF–COSY experiment.

the only drawback of a loss of a factor 2 in the peak intensities.

NOESY

The basic experimental scheme is given in fig. 9 (Macura & Ernst 1981).

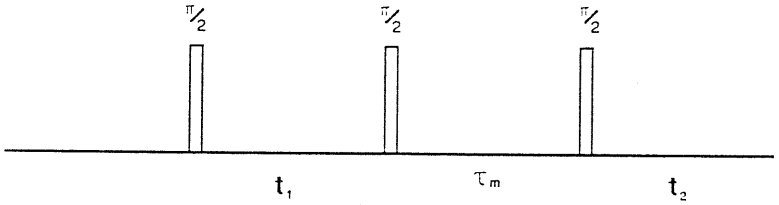

Fig. 9 Basic scheme of a NOESY experiment.

The evolution of the relevant magnetization terms (neglegting J–coupling) under the influence of cross–relaxation is described by the following equation:

$$\vec{M}^+(t_1, \tau_m, t_2) = -exp(L^+ t_2) exp(-R\tau_m) exp(L^+ t_1) \vec{M}^0$$

where

$$\vec{M}^+ = \begin{pmatrix} M_{ix} + iM_{iy} \\ M_{jx} + iM_{jy} \\ \vdots \\ M_{nx} + iM_{ny} \end{pmatrix},$$

$\vec{M}^0$ is the equilibrium magnetization vector

$$\vec{M}^0 = \begin{pmatrix} M^0_{1z} \\ M^0_{2z} \\ \vdots \\ M^0_{nz} \end{pmatrix},$$

$$L^+ = i\Omega - \Lambda$$

and where Ω is the diagonal matrix containing the chemical shift terms (i.e. $\Omega_{lm} = \delta_{lm}\omega_{lm}$) and Λ is also diagonal and contains the transverse relaxation rates (i.e. $\Lambda_{lm} = \delta_{lm}\frac{1}{T_{2l}}$) and R is the relaxation matrix described before. After 2D FT a spectrum is obtained in which the crosspeaks give information on the dipolar intramolecular coupling. Since this interaction dies off with the sixth power of the dipole–dipole distance, the appearance of a crosspeak indicates proximity in space. Moreover the integrated peak intensity depends on τ_m (showing a build–up and a decay), on the rotational correlation time τ_c leading to peaks of opposite sign in the slow ($\omega_0\tau_c \gg 1$) and fast ($\omega_0\tau_c \ll 1$) motion limit and most important of all the interatomic distance can be calculated. During the same pulse and delay sequence of pulses and delays other coherences develop in the system in the presence of J–couplings as shown by a complete density matrix treatment like the one previously shown for the DQF–COSY experiment. Part of these unwanted contributions to the crosspeak intesities can be rejected with the appropriate phase cycling (Bodenhausen et al. 1983) while those unaffected by this procedure are discarded by a random variation of τ_m around the desired value so that the intensity of the J–coupling peaks averages to 0.

TOCSY

Before discussing this experiment it is useful to introduce the average Hamiltonian theory (Haeberlen U. & Waugh J. S. 1968, Ernst et al. 1989). The starting question is the following: can we replace the actual time dependent Hamiltonian $\mathrm{H}(t)$ with some kind of average evolution operator? The answer is yes if we are interested only in the state of the system at a certain time t_c disregarding the way the system has come to this state and if the requirement that $U(t_c) = E$ is fulfilled. We can show this and compute explicitly the average Hamiltonian. Suppose a piecewise constant Hamiltonian, the evolution operator can be written in the following way (we are only interested in the time t_c):

$$U(t_c) = exp(-i\mathrm{H}_n t_n) \ldots exp(-i\mathrm{H}_1 t_1)$$

where Hamiltonians are expressed for simplicity in $\hbar$ units. If we remember the

Baker–Campbell–Hausdorff relation:

$$exp(A)exp(B) = exp((B+A) + \frac{1}{2}([B,A]) + \frac{1}{12}([B,[B,A]] + [[B,A],A]) + \ldots$$

we can write the evolution operator at t_c using an "average" Hamiltonian

$$U(t_c) = exp(-i\overline{\mathbf{H}}t_c).$$

$\overline{\mathbf{H}}$ can be computed making use of the following expansion:

$$\overline{\mathbf{H}} = \overline{\mathbf{H}}^0 + \overline{\mathbf{H}}^1 + \ldots$$

where:

$$\overline{\mathbf{H}}^0 = \frac{1}{t_c}(\mathbf{H}_1 t_1 + \mathbf{H}_2 t_2 + \ldots)$$

$$\overline{\mathbf{H}}^1 = \frac{i}{2t_c}([\mathbf{H}_2 t_2, \mathbf{H}_1 t_1] + [\mathbf{H}_3 t_3, \mathbf{H}_1 t_1] + \ldots)$$

$$\vdots$$

We can neglect higher order terms if $\|\mathbf{H}_i t_i\| \ll 1$. Usually the time dependent Hamiltonian (produced for instance by a sequence of pulses) does not fulfill this requirement so that we have to transfer the time dependence on the static Hamiltonian. We can do this using a reference system "toggling" around with the time dependent Hamiltonian where the previous static Hamiltonian has become time dependent without losing the feature of being "weak". In a more formal way we start with an Hamiltonian of the type:

$$\mathbf{H}(t) = \mathbf{H}_0 + \mathbf{H}_1(t)$$

whose corresponding evolution operator is:

$$U(t) = \mathbf{T}exp[-i\int_0^t (\mathbf{H}_0 + \mathbf{H}_1(t\prime))]dt\prime$$

where $\mathbf{T}$ is the Dyson time–ordering operator. We want to separate the static and time dependent Hamiltonian by writing the evolution operator as a product

$$U(t) = U_1(t)U_0(t)$$

with

$$U_1(t) = \mathbf{T}exp(-i\int_0^t \mathbf{H}_1(t_1)dt_1),$$

$$U_0(t) = \mathbf{T}exp(-i\int_0^t \tilde{\mathbf{H}}_0(t_1)dt_1)$$

and

$$\tilde{\mathbf{H}}_0(t_1) = U_1^{-1}(t_1)\mathbf{H}_0 U_1(t_1).$$

Suppose that $U_1(t_c) = E$, than we can write explicitly the first terms of the average Hamiltonian expansion:

$$\overline{\mathbf{H}}_0^0 = \frac{1}{t_c}\int_0^{t_c} \tilde{\mathbf{H}}_0(t_1)dt_1$$

$$\overline{\mathbf{H}}_0^1 = \frac{-i}{2t_c}\int_0^{t_c} dt_2 \int_0^{t_2} dt_1[\tilde{\mathbf{H}}_0(t_2), \tilde{\mathbf{H}}_0(t_1)]$$

$$\vdots$$

With this result we can discuss the TOCSY experiment starting from what is called an ideal TOCSY Hamiltonian:

$$\mathbf{H} = \sum_{ij} \frac{1}{2} J_{ij} \vec{I}_i \cdot \vec{I}_j$$

In order to reach such an effective we should be able to suppress the chemical shift terms in the actual Hamiltonian (i.e. $\mathbf{H}_{c.s.} = \sum_i \Delta\omega_i I_{iz}$). Average Hamiltonian theory offers the tool to design the suitable pulse sequence. It has been shown (Levitt et al. 1983) that the so called MLEV 16 sequence, composed by 16 pulses ABBA BBAA BAAB AABB, being A a π composite pulse around y–axis (A $= \frac{\pi}{2}_{-y}\pi_x\frac{\pi}{2}_{-y}$) and B its phase reverted analogue (B $= \frac{\pi}{2}_{y}\pi_{-x}\frac{\pi}{2}_{y}$) is able to average to 0 the chemical shift term having a good tolerance on any kind of pulse imperfection (e. g. phase, flip angle). The demonstration relies however on the assumption that the imperfections (for instance on the pulse duration) are the same in any pulse of the sequence. The addition of another π pulse with alternating phase was found to correct to higher accuracy residual imperfections (Bax & Davis 1985).

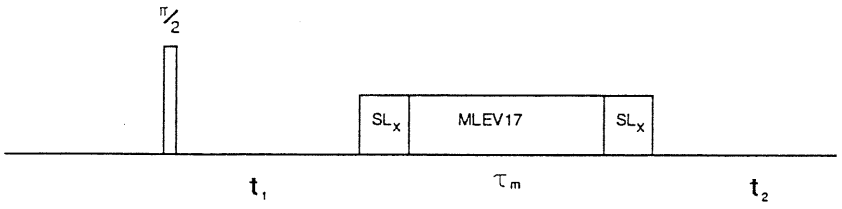

Fig. 10 Experimental scheme of TOCSY. Explanation is given in the text.

The experimental scheme is shown in fig. 10.

The two spin-lock periods at the beginning and at the end of the mixing period are devoted to defocus all the magnetization not parallel to the x–axis. An improvement to this scheme has been proposed (Griesinger et al. (1988)), two delays are inserted in the composite π pulse between the x– and y–pulses. The length of the two flanking periods is chosen in order to cancel the rotating frame NOE peaks developing during the TOCSY mixing period (Bothner–By et al. 1988).

Once an effective TOCSY Hamiltonian is reached the explicit calculation of the spin system evolution is not really straightforward and, up to now, analytical formulas are available only for a limited class of cases. The evocative name of "collective spin modes" (Braunschweiler & Ernst 1983) doesn't give any clue to extend the considerations made on the very simple two–spin system. Numerical calculations were performed for the amino–acid spin systems (Cavanagh et al. 1990) assuming definite values of the J–coupling constant. However, since the quantitative information is not directly available, we want just to discuss the appearance of the spectra obtained. All the peaks are in pure 2D absorption mode and the information they bear depends mainly on the length of the mixing period:

1) for a short τ_{mix} only direct connectivities will appear and the topology of the spectrum will be the same as that of a COSY spectrum,

2) for a long τ_{mix}, in the most favorable cases all the resonances belonging to the same spin system are connected by a crosspeak. The usefulness of this feature is appearent if we think that every amino–acid constitutes an autonomous spin–system.

Experimental

Nisin was purchased from Koch–Light Ltd. (lot n.00988E spec. act. 3700 u/mg) and dissolved in mixtures of water and deuterated (D 99.8%) trifluoroethanol (TFE) purchased from Janssen Chimica. The Nisin concentration was in the range 2–5 mM and the pH of the samples was always around 3.5. The maximum feasible concentration of TFE was searched adding this solvent to Nisin in water until the sample aggregated. 80% was the maximum ratio of TFE to total volume compatible with the range of concentrations mentioned above. 1D NMR spectra were recorded on a Bruker WM–200 200 MHz spectrometer in order to check the quality of the signal during this procedure. The other 1D– and 2D–spectra were recorded on a Bruker AM–400 400 MHz spectrometer at room temperature 25°C and 5°C. The list of the relevant parameters of all the experiments performed is given in table I together with an explanation of the symbols used.

The suppression of the water signal was achieved alternatively by means of the DANTE pulse sequence (Morris & Freeman 1978) or irradiating before and during the experiment. In both cases the decoupler was used.The standard phase cycling supported by the Bruker aquisition software was employed in all the experiments and all the spectra were recorded in the TPPI mode (Bodenhausen et al. 1980). All the spectra were zero–filled and multiplied by a window function (usually a shifted sine bell or a shifted sine square bell) in both dimensions before Fourier transformation in order to remove ripples and enhance the resolution. The shift was optimized for best appearance of the spectrum.

THE ASSIGNMENT OF THE 1H SPECTRUM

Two complete sets of assignments were obtained at 5°C and 25°C employing TOCSY, DQF–COSY and NOESY spectra with different mixing times.

Par	NOE1	NOE2	NOE3	NOE4	NOE5	CO1	TOC1	TOC2	TOC3
DW	100	100	100	100	100	100	100	100	100
SW	5000	5000	5000	5000	5000	5000	5000	5000	5000
NP(1)	256	256	512	512	512	256	512	512	512
NP(2)	2048	4096	2048	2048	2048	4096	4096	2048	2048
Temp	298	298	278	278	278	298	298	278	278
τ_{mix}	200	250	150	300	600	***	25	12	64
Ssup	Irr.	Irr.	D.s.	D.s.	D.s.	Irr.	D.s.	D.s.	D.s.
AQ(1)	.025	.025	.051	.051	.051	.025	.051	.051	.051
AQ(2)	.205	.410	.205	.205	.205	.410	.410	.205	.205
RD	1	1	1	1	1	1	1	1	1
NS	112	64	48	48	48	64	88	48	48
DS	4	4	4	4	4	4	4	4	4
DP	25L	25L	9H	9H	9H	25L	8H	9H	9H
DM	N	N	I	I	I	N	I	I	I

TABLE I. A summary of the experiments performed; NOEn stands for NOESY, COn for COSY and TOCn for TOCSY. The relevant parameters are explained below:

DW = Dwell time (in (μsec)) in both dimensions

SW = Spectral width (in Hz) in both dimensions

NP(i) = Number of points in the i–th dimension

Temp = Temperature in Kelvin degrees

τ_{mix} = Duration of the mixing time in milliseconds

Ssup = Solvent suppression: Irr. means achieved by irradiation on the decoupler and D.s. by means of the DANTE sequence

AQ(i) = Aquisition time in the i–th dimension in seconds

RD = Relaxation delay in seconds

NS = Number of scans

DS = Number of dummy scans

DP = Decoupler power in decibel attenuation on two different levels: H is 15 Watt and L is 0.2 Watt.

DM = Detection mode: I means Inverse and N normal.

The major difficulties came from occasional overlap of resonances, present also for such a small molecule, impurities and bleaching out due to the irradiation of the solvent. Recording spectra at different temperatures partially solved

Residue	nr.	atom	δ_{Water}	δ_{TFE}	$\delta_{Water} - \delta_{TFE}$
Ile	1	N	****	8.03	****
Ile	1	C_α	4.15	4.07	0.08
Ile	1	C_β	2.14	2.03	0.11
Ile	1	$C_{\gamma 1}$	1.57	1.54	0.03
Ile	1	$C_{\gamma 2}$	1.31	1.19	0.12
Ile	1	$C_{\gamma M}$	1.12	0.99	0.13
Ile	1	C_δ	0.99	0.91	0.08
Dhb	2	N	10.08	9.81	0.27
Dhb	2	C_β	6.63	6.69	-0.06
Dhb	2	$C_{\gamma M}$	1.85	1.75	0.10
Alas	3	N	8.42	7.70	0.72
Alas	3	C_α	4.61	4.53	0.08
Alas	3	$C_{\beta 1}$	3.31	3.27	0.04
Alas	3	$C_{\beta 2}$	3.17	2.95	0.22
Ile	4	N	7.91	8.40	-0.49
Ile	4	C_α	4.38	4.07	0.31
Ile	4	C_β	2.11	1.88	0.23
Ile	4	$C_{\gamma 1}$	1.40	1.38	0.02
Ile	4	$C_{\gamma 2}$	1.19	1.05	0.14
Ile	4	$C_{\gamma M}$	0.95	0.85	0.10
Ile	4	C_δ	0.86	0.71	0.15
Dha	5	N	10.11	8.81	1.30
Dha	5	$C_{\beta 1}$	5.56	5.94	-0.38
Dha	5	$C_{\beta 2}$	5.46	5.39	0.07
Leu	6	N	9.14	8.52	0.62
Leu	6	C_α	4.45	4.03	0.42
Leu	6	C_β	1.76	1.67	0.09
Leu	6	C_γ	1.69	1.50	0.19
Leu	6	C_δ	0.94	1.02	-0.08

TABLE I.Assignments of the resonances of Nisin at 500 Mhz in TFE/water mixtures and water (Slijper et al. 1989) at 5°C (In this scale TFE residual peak is at 3.81 ppm.).

the problems connected with the solvent since this underwent a large shift in its resonance position. An example of overlap is reported in fig. 11 showing the amide–amide region of a NOESY spectrum.

The intense peak at 7.79–8.53 ppm is due to the following couples of residues: 25–26, 26–27 and 27–28. In such cases several possible assignments were formulated

Residue	nr.	atom	δ_{Water}	δ_{TFE}	$\delta_{Water} - \delta_{TFE}$
Alas	7	N	8.33	8.00	0.33
Alas	7	C_α	4.54	4.89	-0.35
Alas	7	$C_{\beta 1}$	3.05	3.06	-0.01
Alas	7	$C_{\beta 2}$	2.94	2.73	0.21
Abas	8	N	9.04	8.90	0.14
Abas	8	C_α	5.16	4.80	0.36
Abas	8	C_β	3.62	3.44	0.18
Abas	8	$C_{\gamma M}$	1.32	1.19	0.13
Pro	9	C_α	4.46	4.27	0.19
Pro	9	$C_{\beta 1}$	2.50	2.30	0.20
Pro	9	$C_{\beta 2}$	1.82	1.80	0.02
Pro	9	$C_{\gamma 1}$	2.20	2.02	0.18
Pro	9	$C_{\gamma 2}$	1.97	1.80	0.17
Pro	9	C_δ	3.46	3.59	-0.13
Pro	9	C_δ	3.46	3.31	0.15
Gly	10	N	8.74	8.63	0.11
Gly	10	C_{α_1}	4.50	4.33	0.17
Gly	10	C_{α_2}	3.53	3.54	-0.01
Alas	11	N	7.92	7.81	0.11
Alas	11	C_α	4.04	3.97	0.07
Alas	11	$C_{\beta 1}$	3.66	3.56	0.10
Alas	11	$C_{\beta 2}$	3.03	2.92	0.11
Lys	12	N	8.80	8.43	0.37
Lys	12	C_α	4.32	4.31	0.01
Lys	12	$C_{\beta 1}$	1.82	1.72	0.10
Lys	12	$C_{\beta 2}$	1.73	1.72	0.01
Lys	12	C_γ	1.39	1.43	-0.04
Lys	12	C_δ	1.54	1.63	-0.09
Lys	12	C_ϵ	3.02	2.89	0.13
Lys	12	N_ζ	7.65	7.50	0.15

TABLE I. Continued.

and further confirmations in the spectra (both NOESY and TOCSY) were searched for until only one assignment could fit all the data. In particular the alpha–amide region of the NOESY spectrum is very significant since a crosspeak between adjacent residues is always expected. The COSY spectrum was not of great help in this procedure since, due to the antiphase splittings and possible cancellation of overlapping mismatching peaks, several situations were unclear and furthermore

Residue	nr.	atom	δ_{Water}	δ_{TFE}	$\delta_{Water} - \delta_{TFE}$
Abas	13	N	8.63	7.95	0.68
Abas	13	C_{α}	4.64	4.56	0.08
Abas	13	C_{β}	3.67	3.57	0.10
Abas	13	$C_{\gamma M}$	1.36	1.24	0.12
Gly	14	N	8.35	8.09	0.26
Gly	14	C_{α_1}	4.18	4.17	0.01
Gly	14	C_{α_2}	4.08	3.91	0.17
Ala	15	N	8.77	7.95	0.82
Ala	15	C_{α}	4.24	4.11	0.13
Ala	15	$C_{\beta M}$	1.49	1.37	0.12
Leu	16	N	8.66	8.09	0.57
Leu	16	C_{α}	4.36	4.13	0.23
Leu	16	C_{β}	1.78	1.70	0.08
Leu	16	C_{γ}	1.67	1.55	0.12
Leu	16	C_{δ}	0.91	0.81	0.10
Met	17	N	7.85	7.84	0.01
Met	17	C_{α}	4.74	4.39	0.35
Met	17	$C_{\beta 1}$	2.34	2.17	0.17
Met	17	$C_{\beta 2}$	2.13	2.08	0.05
Met	17	$C_{\gamma 1}$	2.64	2.57	0.07
Met	17	$C_{\gamma 2}$	2.43	2.48	-0.05
Met	17	$C_{\epsilon M}$	2.11	2.04	0.07
Gly	18	N	8.20	7.85	0.35
Gly	18	C_{α_1}	4.11	4.06	0.05
Gly	18	C_{α_2}	3.85	3.77	0.08
Alas	19	N	7.74	7.50	0.24
Alas	19	C_{α}	4.52	4.36	0.16
Alas	19	$C_{\beta 1}$	3.01	3.04	-0.03
Alas	19	$C_{\beta 2}$	2.93	2.84	0.09

TABLE I. Continued.

most of the information was already contained in the TOCSY spectra with short mixing time. The particular case cited will be discussed also later. Impurities were also present; all the spectra and possible connectivities were checked before discarding a peak. In several cases a crosspeak was found only in the TOCSY while it was missing in the NOESY spectrum so that it was attributed to some small molecule still present in the sample. The cases different from these will be

Residue	nr.	atom	δ_{Water}	δ_{TFE}	$\delta_{Water} - \delta_{TFE}$
Asn	20	N	8.70	8.33	0.37
Asn	20	C_α	4.66	4.57	0.09
Asn	20	$C_{\beta 1}$	2.86	2.74	0.12
Asn	20	$C_{\beta 2}$	2.82	2.74	0.08
Asn	20	$N\gamma_1$	7.72	7.37	0.35
Asn	20	$N\gamma_2$	7.05	6.62	0.43
Met	21	N	8.45	7.99	0.46
Met	21	C_α	4.54	4.45	0.09
Met	21	$C_{\beta 1}$	2.16	2.10	0.06
Met	21	$C_{\beta 2}$	2.01	1.93	0.08
Met	21	$C_{\gamma 1}$	2.63	2.50	0.13
Met	21	$C_{\gamma 2}$	2.53	2.39	0.14
Met	21	$C_{\epsilon M}$	2.11	2.00	0.11
Lys	22	N	8.58	7.98	0.60
Lys	22	C_α	4.31	4.17	0.14
Lys	22	$C_{\beta 1}$	1.87	1.75	0.12
Lys	22	$C_{\beta 2}$	1.74	1.75	-0.01
Lys	22	C_γ	1.45	1.45	0.00
Lys	22	C_δ	1.53	1.64	-0.11
Lys	22	C_ϵ	3.02	2.91	0.11
Lys	22	N_ζ	7.65	7.50	0.15
Abas	23	N	9.01	8.41	0.60
Abas	23	C_α	5.13	4.89	0.24
Abas	23	C_β	3.58	3.39	0.19
Abas	23	$C_{\gamma M}$	1.37	1.24	0.13
Ala	24	N	8.34	8.17	0.17
Ala	24	C_α	4.65	4.52	0.13
Ala	24	$C_{\beta M}$	1.46	1.38	0.08
Abas	25	N	9.32	8.53	0.79
Abas	25	C_α	4.77	4.72	0.05
Abas	25	C_β	3.55	3.42	0.13
Abas	25	$C_{\gamma M}$	1.47	1.33	0.14

TABLE I. Continued.

mentioned later. The procedure used to assign the spectra was slightly different from the one proposed by Wütrich (1986) in that ambiguities during spin systems identification were solved by comparison with NOESY spectra.

a) Spin system identification.

Residue	nr.	atom	δ_{Water}	δ_{TFE}	$\delta_{Water} - \delta_{TFE}$
Alas	26	N	7.90	7.79	0.11
Alas	26	C_α	3.86	3.77	0.09
Alas	26	$C_{\beta 1}$	3.44	3.36	0.08
Alas	26	$C_{\beta 2}$	2.70	2.61	0.09
His	27	N	8.86	8.53	0.33
His	27	C_α	5.03	4.85	0.18
His	27	$C_{\beta 1}$	3.38	3.32	0.06
His	27	$C_{\beta 2}$	3.08	2.97	0.11
His	27	C_2	8.66	8.38	0.28
His	27	C_4	7.34	7.14	0.20
Alas	28	N	8.04	7.79	0.25
Alas	28	C_α	4.44	4.29	0.15
Alas	28	$C_{\beta 1}$	3.72	3.54	0.18
Alas	28	$C_{\beta 2}$	2.71	2.67	0.04
Ser	29	N	8.60	8.12	0.48
Ser	29	C_α	4.50	4.38	0.12
Ser	29	C_β	3.86	3.80	0.06
Ser	29	C_β	3.86	3.74	0.12
Ile	30	N	8.33	7.71	0.62
Ile	30	C_α	4.19	4.08	0.11
Ile	30	C_β	1.86	1.75	0.11
Ile	30	$C_{\gamma 1}$	1.40	1.31	0.09
Ile	30	$C_{\gamma 2}$	1.18	1.06	0.12
Ile	30	$C_{\gamma M}$	0.87	0.77	0.10
Ile	30	C_δ	0.86	0.77	0.09
His	31	N	8.82	8.12	0.70
His	31	C_α	4.78	4.70	0.08
His	31	$C_{\beta 1}$	3.23	3.17	0.06
His	31	$C_{\beta 2}$	3.18	3.06	0.12
His	31	C_2	8.62	8.38	0.24
His	31	C_4	7.30	7.14	0.16

TABLE I. Continued.

First of all characteristic patterns of crosspeaks corresponding to particular spin systems were looked for in the TOCSY spectra with longer mixing times. Hereafter a list of this patterns (together with the multiplicity of the corresponding residues) is given:

1) long side chain systems containing one or more methyl groups (3 Isoleucines,

Residue	nr.	atom	δ_{Water}	δ_{TFE}	$\delta_{Water} - \delta_{TFE}$
Val	32	N	8.50	7.96	0.54
Val	32	C_α	4.18	4.09	0.09
Val	32	C_β	2.09	2.01	0.08
Val	32	$C_{\gamma M}$	0.97	0.87	0.10
Dha	33	N	9.84	9.06	0.78
Dha	33	$C_{\beta 1}$	5.73	5.86	-0.13
Dha	33	$C_{\beta 2}$	5.73	5.65	0.08
Lys	34	N	8.34	7.90	0.44
Lys	34	C_α	4.32	4.39	-0.07
Lys	34	$C_{\beta 1}$	1.85	1.89	-0.04
Lys	34	$C_{\beta 2}$	1.74	1.75	-0.01
Lys	34	C_γ	1.37	1.42	-0.05
Lys	34	C_δ	1.48	1.63	-0.15
Lys	34	C_ϵ	3.02	2.90	0.12
Lys	34	N_ζ	7.65	7.50	0.15

TABLE I. Continued.

2 Leucines and 1 Valine),

2) systems with unusual chemical shifts (1 dehydrobutyrine and 2 dehydroalanines),

3) 'AMX' systems (5 D–Alanines and 1 L–Alanine in the Lanthionine and Methyl–lanthionine residues, 1Asparagine, 2 Histidines and 1 Serine),

4) 'AMX' systems with a methyl group (4 methylated Alanines in the Lanthionine and Methyl–lanthionine residues),

5) long side chains with no methyl groups (1 Proline, 3 Lysines and 2 Methionines),

6) 'A_2' systems (3 Glycines),

7) 'A_2' systems with a methyl group (2 Alanines).

1) The crosspeaks in the alpha–methyl region of the spectra (fig. 12) allow a straightforward identification of the alpha proton chemical shifts. However, since the latter have very close values for all the three isoleucines and valine an analysis of the whole crosspeak network was necessary. The crosspeaks appear much more

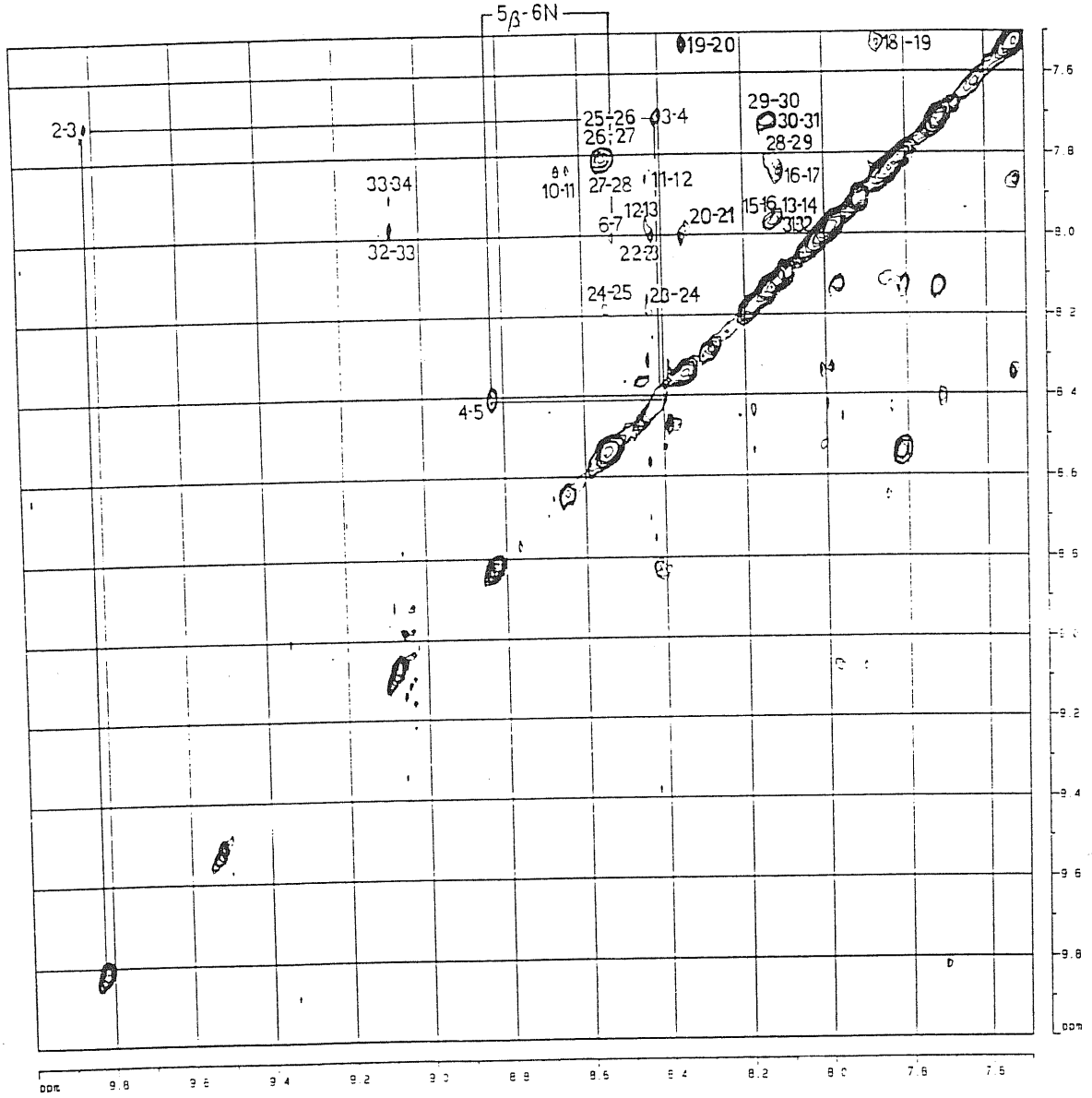

Fig. 11 NOESY spectrum NO3 (for the list of parameters see table I)

dispersed in the methyl–methyl region (fig. 13) and also the amide protons gave rise to crosspeaks to the long side chain (fig. 14). Uncertainties due to noise and impurities showing only in the TOCSY spectra were solved by comparison with all the other spectra.

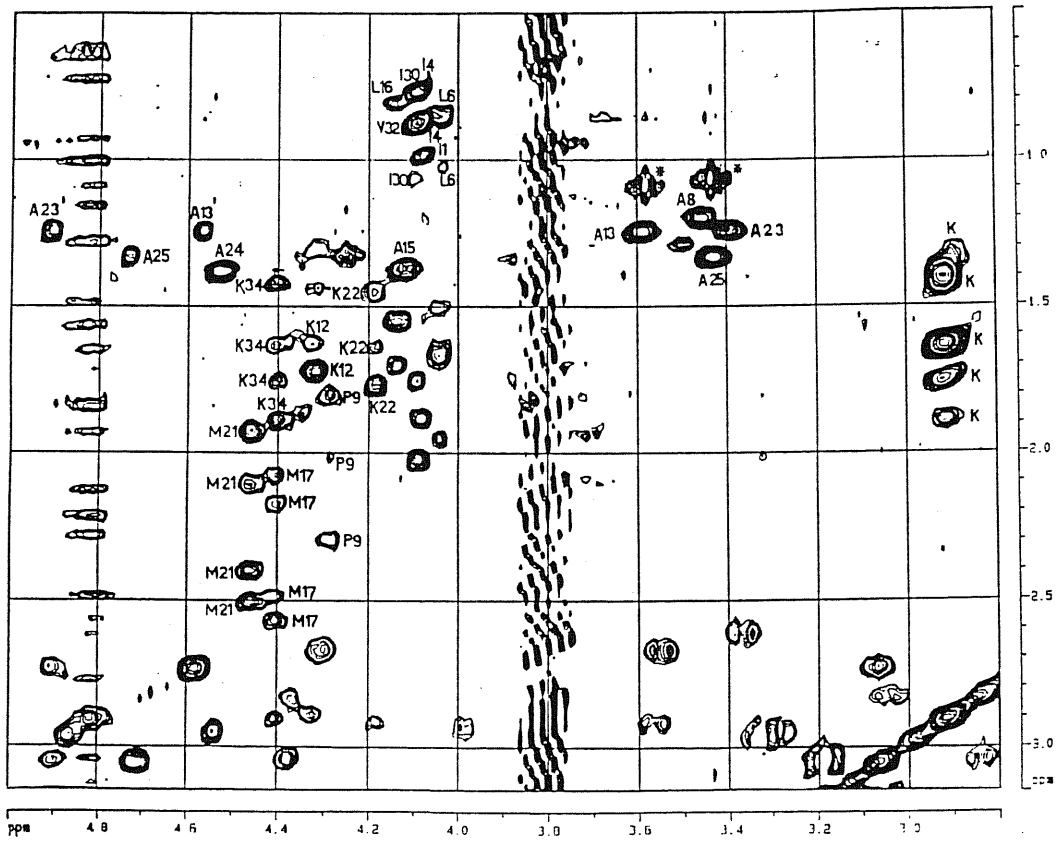

Fig. 12 TOCSY spectrum TO3 (for the list of parameters see table I)

2) This class of residues has unusual chemical shifts, due to the presence of an unsaturated bond, for both the amide– and beta–protons so that it was not difficult to assign their crosspeaks. It is worth noticing that, since these were assigned with the highest degree of reliability they could constitute a "marked" starting point for the sequential analysis to be described later and a check on the

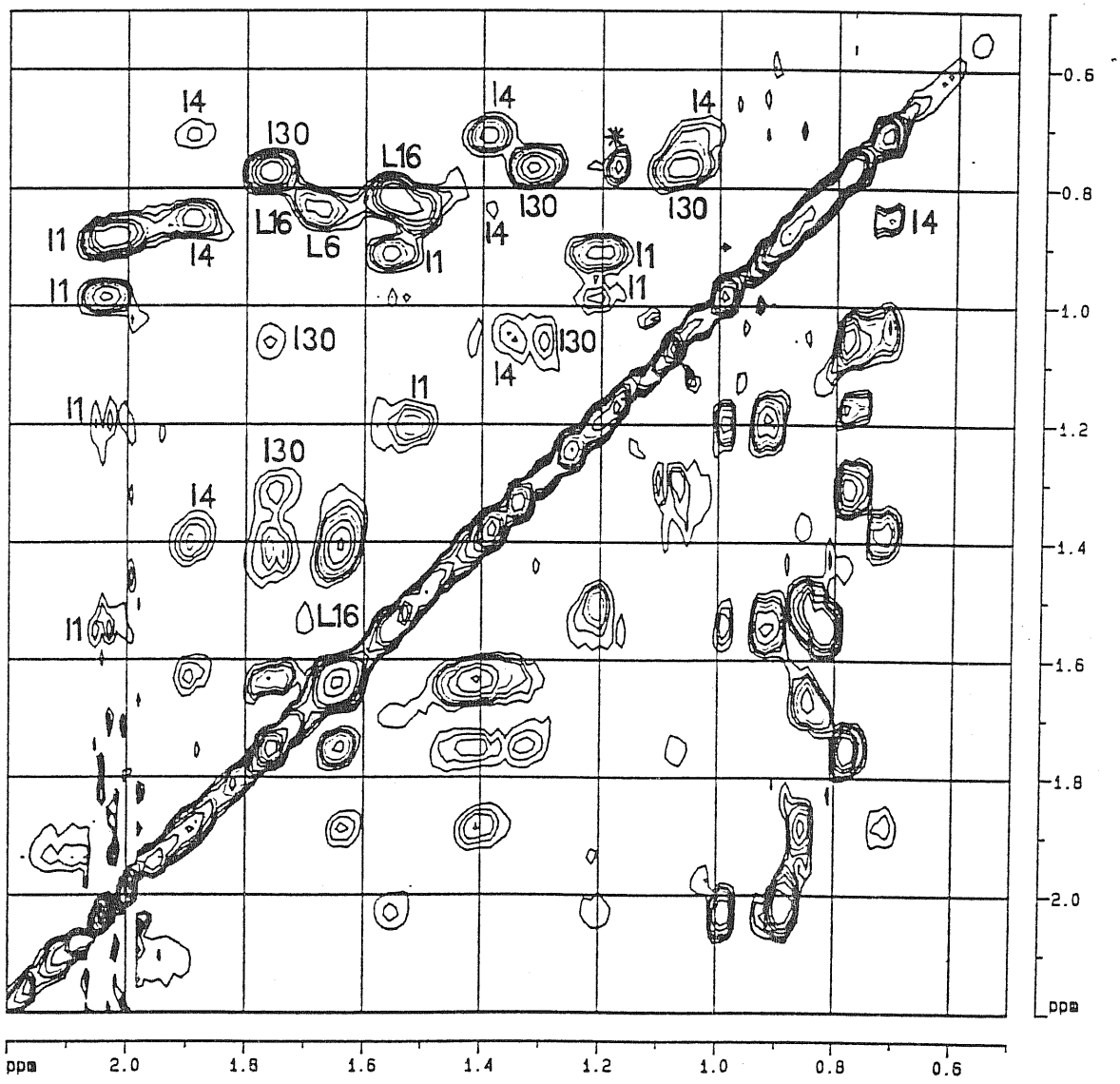

Fig. 13 TOCSY spectrum TO3 (for the list of parameters see table I)

correctness of the sequential walk.

3) This pattern is easily recognizable. First we looked, in correspondence to the alpha region, for the 'AM' and 'AX' crosspeaks and then the presence of a 'MX' crosspeak was the confirmation of this pattern (fig.15). With these three

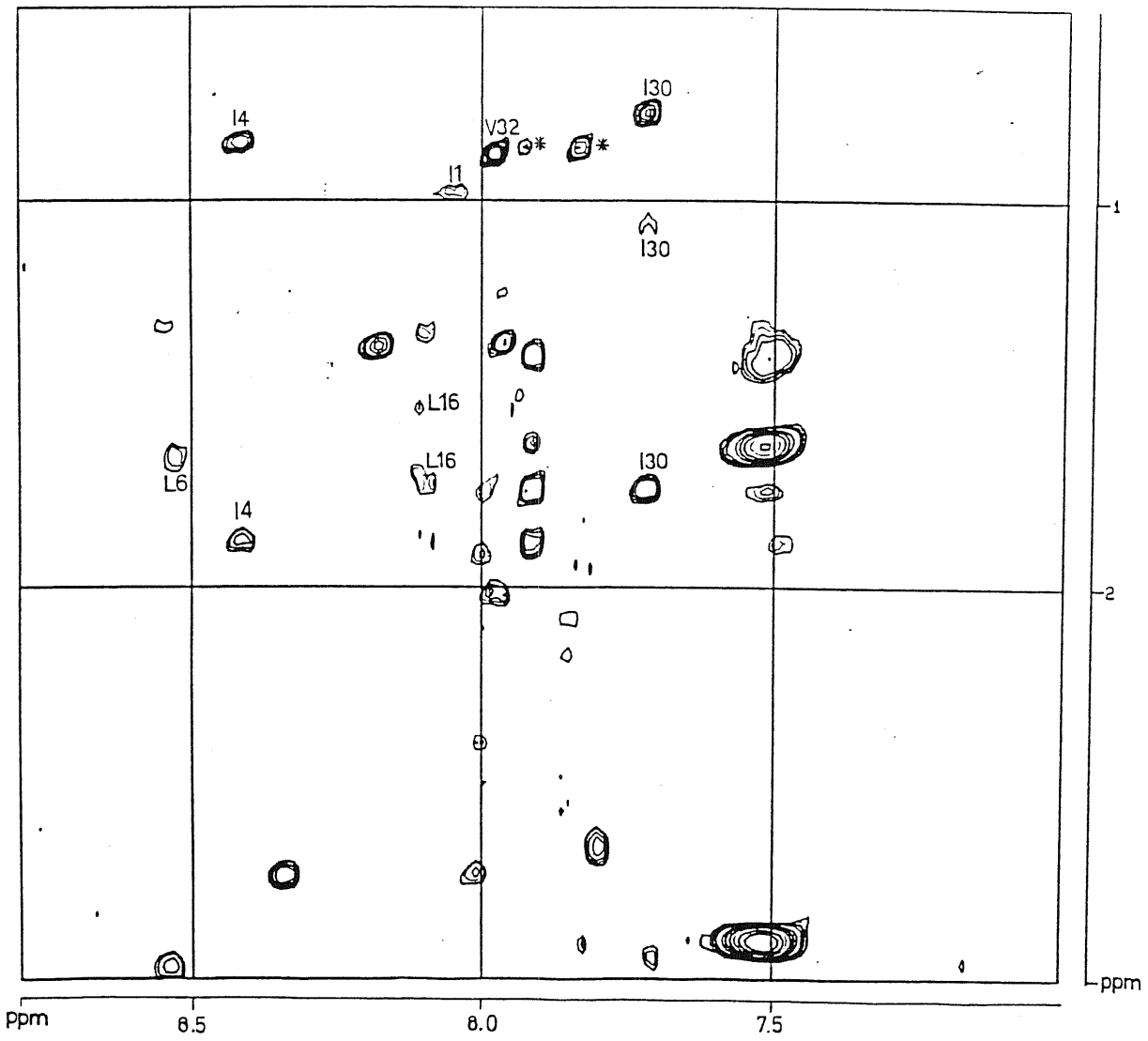

Fig. 14 TOCSY spectrum TO3 (for the list of parameters see table I)

resonances assigned it was not difficult to find the position of the corresponding amide–proton (fig.16). For Histidines and Asparagine the other protons of the amino acid could be assigned in the NOESY spectra.

The beta to methyl crosspeaks are found in a region otherwise empty of the spec-

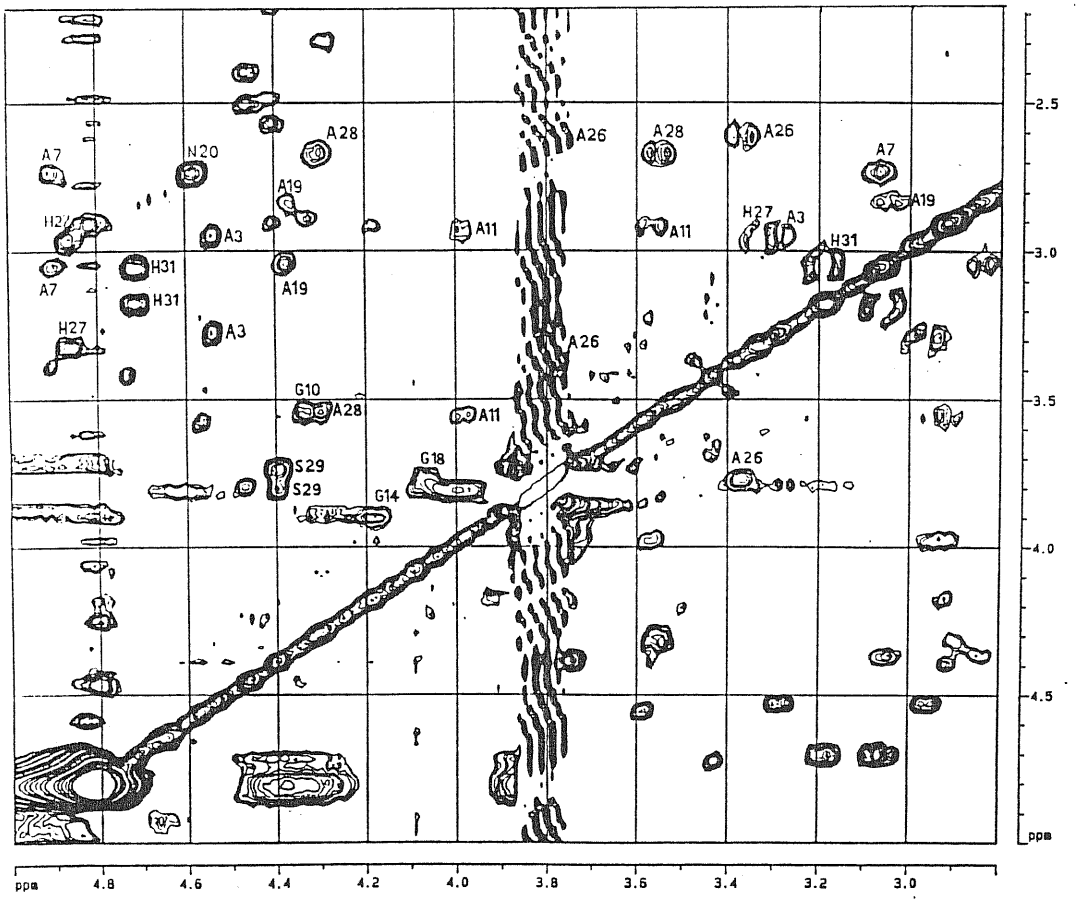

Fig. 15 TOCSY spectrum TO3 (for the list of parameters see table I.

trum (fig. 12), then the alpha region and finally the amide region were analysed. A kind of impurities already observed in the water spectra was also present and it has been indicated by a star in the figures. Problems arised due to the bleaching out of the alpha resonance of $Abas_8$ so that also in the sequential analysis the information involving this residue was almost completely missing.

5) The alpha to beta and to gamma crosspeaks were first detected (fig. 12) then confirmation crosspeaks were investigated in the aliphatic–amide and

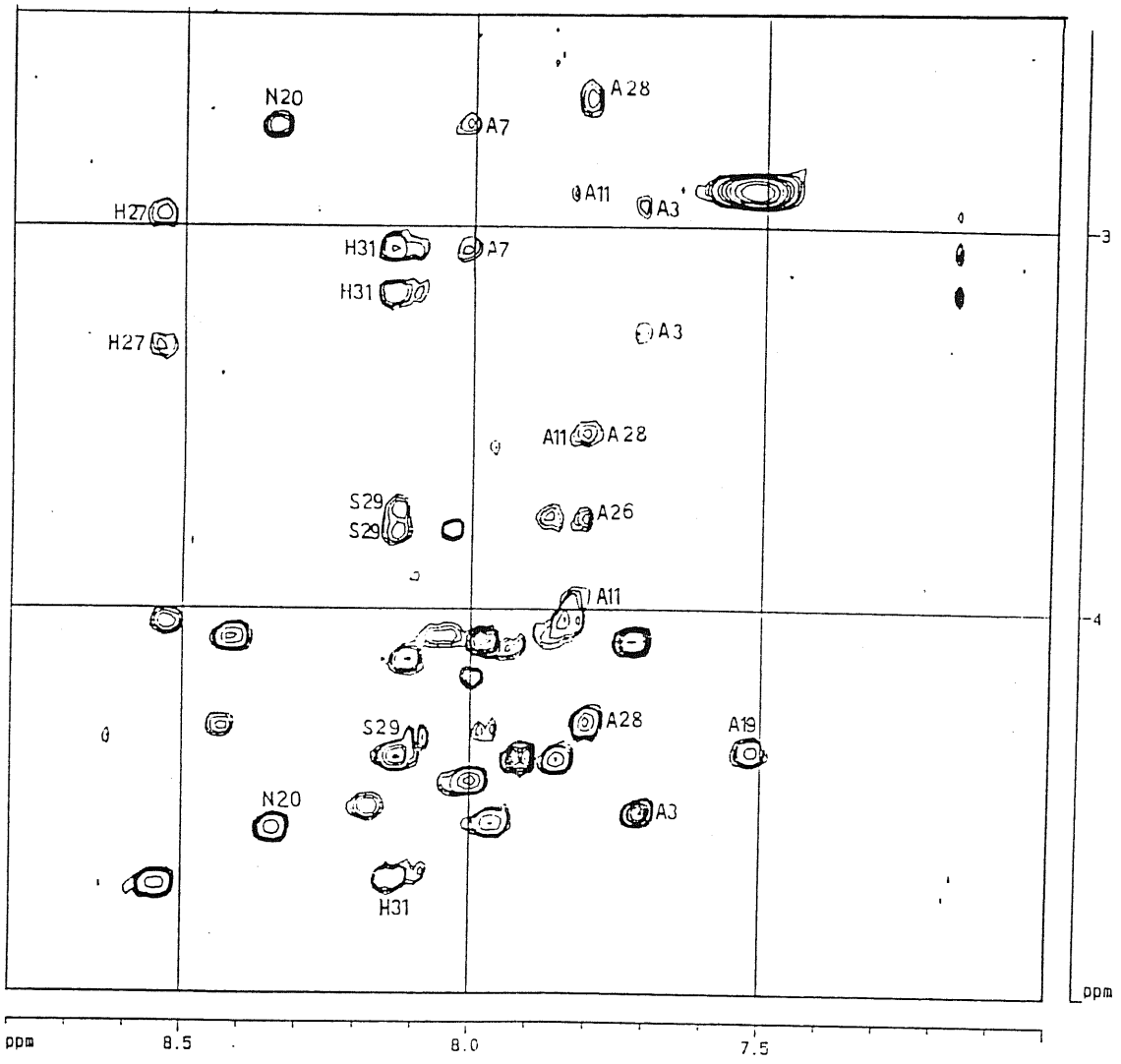

Fig. 16 TOCSY spectrum TO3 (for the list of parameters see table I)

aliphatic–aliphatic regions. A very clear clue to the identification the Lysine spin system was provided by the crosspeaks in correspondence with the epsilon protons that gave the (approximate due to overlap and broadening) position of the side

chain resonances.

6) Glycines were apparent as a strong connectivity in the alpha–alpha region due to geminal coupling (fig. 15). The only necessary check was that this was not part of a larger network. This was easily done and further confirmation came from the amide–alpha region.

7) Alanines were recognized as a strong (due to direct connectivity) crosspeak in the alpha–methyl (fig. 12) region and then confirmed in the amide region.

b) Residue specific assignment.

A summarizing list of the sequential NOE's found in the spectra is shown in table III.

Further confirmations of the assignment were provided by the NOE's between residues kept close in space by the thioether bridges. Most important for the sequential assignment were the amide–amide and alpha–amide regions. A clear example of a short sequential walk in the amide–amide region is given in fig. 11. Similar walks, connecting sequential and intra–residual crosspeaks, could be followed also in the alpha–amide region (fig. 17) and constant comparison between the walks in the two regions permitted to chose among mutually excluding residue specific assignments.

The ambiguities arose from overlap between the crosspeaks of couples of adjacent residues or resonances of adjacent residues (so that their crosspeak was covered by the diagonal) and by bleaching out due to the irradiation of the solvent as mentioned previously. For the sake of clarity an example of how ambiguities can arise and be solved is given in the following. If we consider $Abas_{13}$ and $Abas_{23}$ they are both preceeded by a Lysine and the amide proton resonances of Gly_{14} and Ala_{24} are overlapping so that we cannot distinguish the sequential walks involving the amide protons of residues 12–13–14 and 22–23–24 unless the expected connectivity between an alpha proton of an "AMX" system (or of a Methionine) and the amide of one of the two Lysines is found. Obviously the chance that a crosspeak is due to impurities or noise must always be taken into account as well as the chance that we are confusing long range NOE's with sequential ones, so that all the possible confirmations must be looked for. However the small number of residues in Nisin made all the assignment procedure quite straightforward and two independently performed assignments on the spectra recorded at different temperatures agreed

nr.	residue	N–N	C_α–N	others	non seq
1	I		*	*	
2	O	*		*	4
3	A	*	*	*	5
4	I	*	*	*	2
5	U			*	3,7
6	L	*	*	*	
7	A				5
8	A				
9	P		*	*	
10	G	*	*		
11	A	*	*	*	
12	K	*	*	*	
13	A	*	*	*	20
14	G	*	*	*	
15	A	*		*	17,20
16	L	*	*	*	
17	M				15,19
18	G	*	*	*	
19	A	*	*	*	17
20	N	*	*	*	13,15
21	M		*		
22	K	*	*	*	24
23	A	*	*		27
24	A	*	*	*	22,26
25	A	*	*	*	29
26	A	*		*	24
27	H	*		*	23
28	A	*	*	*	
29	S	*	*	*	25
30	I	*	*	*	
31	H	*	*	*	
32	V	*	*	*	
33	U	*		*	
34	K				

TABLE III. List of sequential connectivities found in the NOESY spectra of Nisin at 5°C. Non adjacent residues connected by one or more crosspeaks are listed in the last column.

completely.

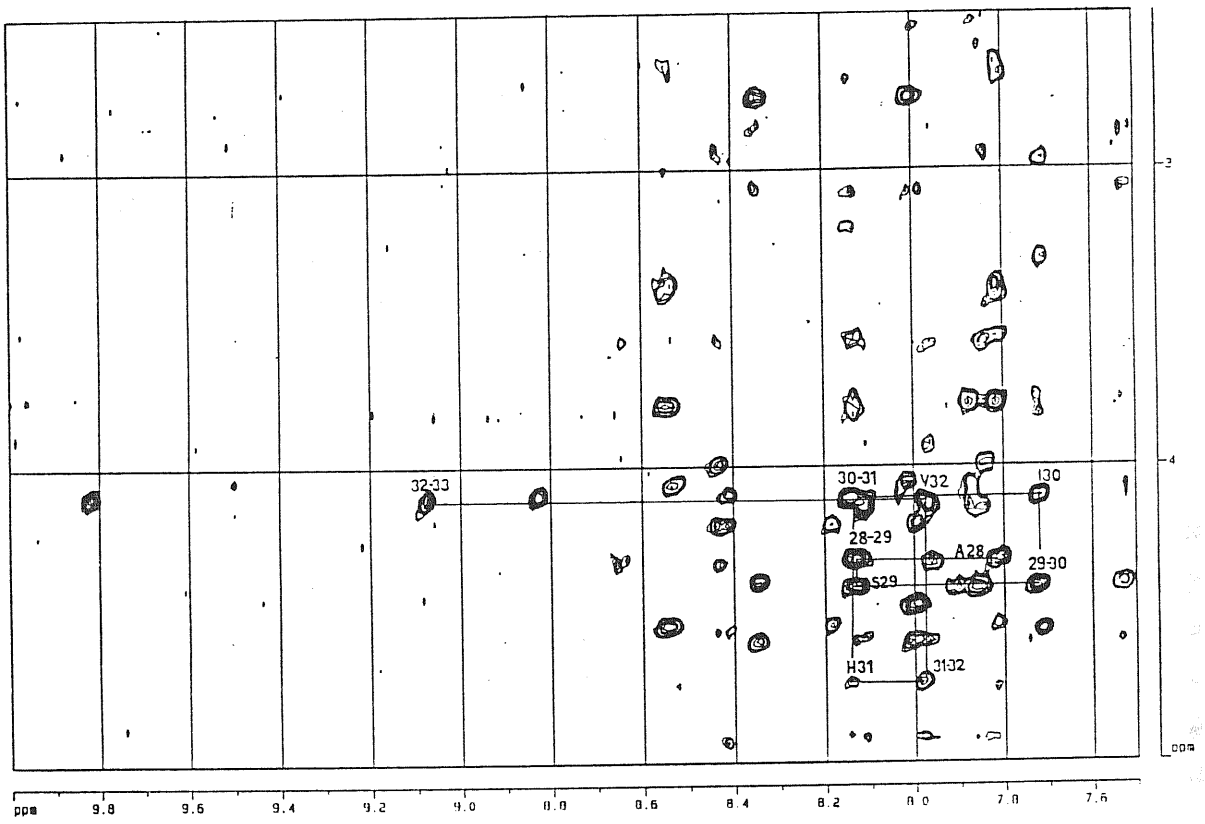

Fig. 17 NOESY spectrum NO3 (for the list of parameters see table I)

Results and discussion

NISIN SPECTRUM IN WATER AND WATER/TFE MIXTURE

Once the assignments for Nisin in water/TFE mixture were obtained the most straightforward thing to do was to compare the chemical shifts with those

reported for Nisin in water. The chemical shifts for the two cases and their difference are reported in table II and the chemical shift difference for amide and alpha protons together with a plot of the hydrophobicity of Nisin is reported in fig.18.

A general feature that is apparent is the overall positive shift of all the resonances. It is interesting to note that the only exceptions worth noticing are found in the first 11 residues. Although it is not possible to correlate this univoquely with physical properties we can try to speculate in two directions assuming either a different local conformation at these residues or a different accessibility and/or affinity for the solvent molecules in the vicinity of the protons under discussion. The overall effect of the solvent change on the resonances can be qualitatively tested on Lysins which have been seen in all preliminary molecular modelling studies to stick out in the solvent (this can also be gleaned by the few inter–residual NOE's involving their long side chain protons). As can be seen, although not always with the same sign, the shifts are very small, so that we can suspect the largest shifts found to be correlated with some micro–environment change (we have obviously discarded ring current effects since the aromatic residues are too far away). At least in water the shifts observed for amide protons relative to their random coil values could be correlated with hydrogen bonding (Wagner et al. 1983) and this could also be the case here for what concerns the Ile_4 amide proton. However, for the time being, these must be regarded as pure speculations.

NOESY SPECTRA AND DISTANCE CONSTRAINTS

All the crosspeaks in the NOESY spectra were integrated using the software installed on the Bruker X32 computer. Three different files corresponding to three different mixing times were prepared for the lower temperature spectra. Obviously the integration was not always straightforward due to complete or partial overlap. We didn't make use of any fitting procedure,but, when it was possible, the total crosspeak intensity was partitioned into different intensities corresponding to each overlapping crosspeak (usually no more than two). Although this procedure can lead to mistakes it was the most reasonable way to take into account the information contained in the Noesy spectra and we are quite confident that no major mistake was introduced. In the following we want to discuss some of the possible

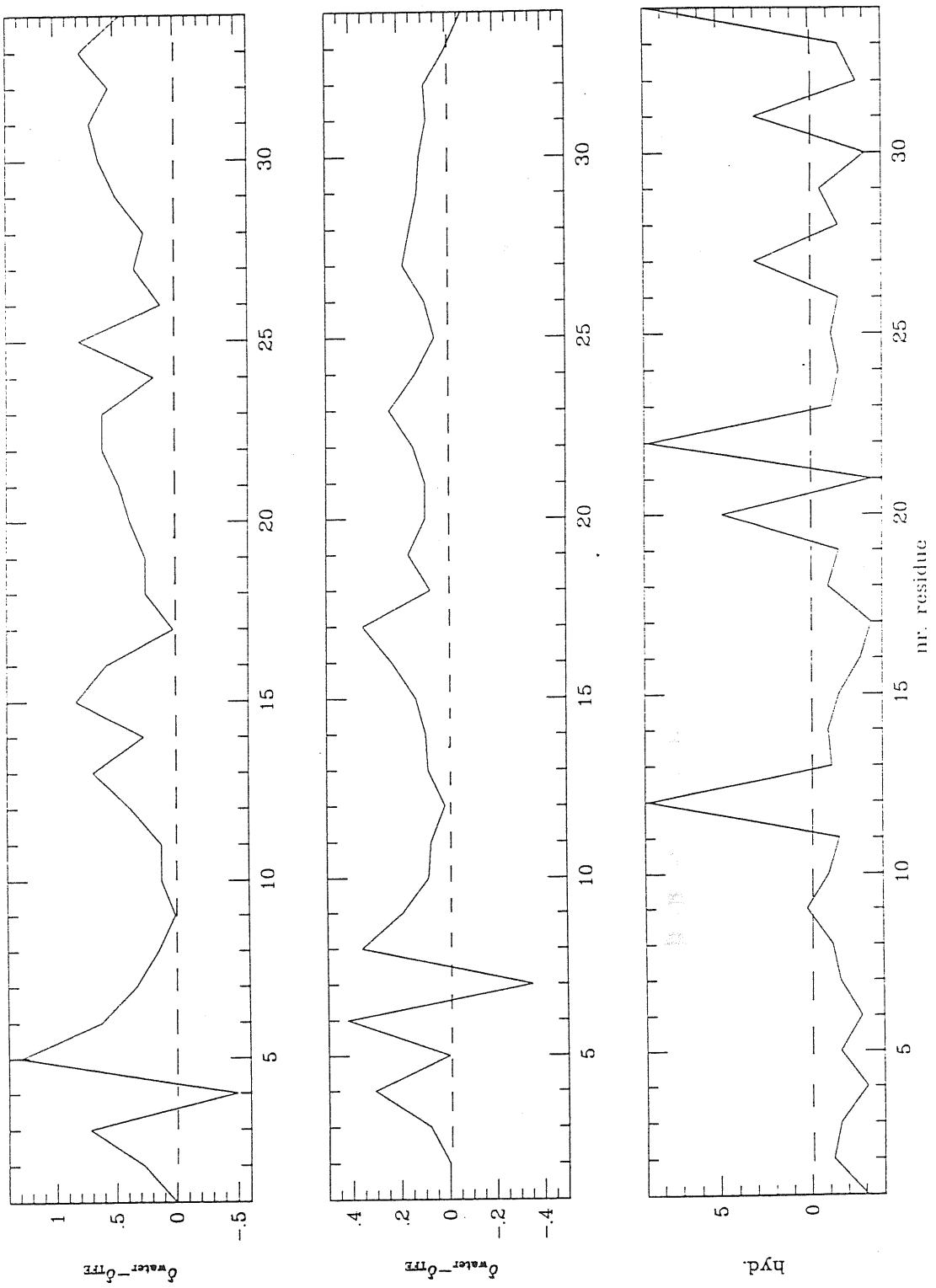

Fig. 18 The chemical shift differences for Nisin in Water and TFE/mixture (amide protons (upper) and alpha protons (middle)) and a hydrophobicity plot (lower) according to Engelman et al. 1986.

errors intrinsic to this procedure and their entity.)

When partial overlap is present the intensities can mismatch the real ones. Anyway due to the $(\frac{1}{r})^6$ dependence of the NOE's intensity a factor 2 in the size of the crosspeak will be reflected in a factor $(\sqrt[6]{\frac{1}{2}})$ in the distance which is usually in the range of uncertainty intrinsic to the experiment.)

A much heavier error would be introduced if we attributed a single crosspeak to two completely overlapping ones, creating a fake connectivity in the molecule. So, when there is any chance to make this mistake, use must be made of all the information available, for instance, in our case, the constraints on the structure posed by the monosulphur bridges. These cases were not frequent anyway . One of the worst, concerning the amide to amide crosspeaks of residues 25–26, 26–27 and 27–28 was already mentioned (these were however resolved in the higher temperature spectrum). In this situation both the knowledge that the above mentioned couples of protons are part of a ring and most of all the very high intensity of the peak (also after partition it was still one of the highest) made the division of this peak into three equally intense peaks a reasonable choice. More complex situations were encountered near the diagonal were it was difficult to divide very large spots into several distinguished peaks. We decided to take only the risk to mistake some intensity of intraresidual crosspeaks discarding every possible interresidual connectivity for the reasons mentioned above. Some more subtle question could arise for resonances overlapping because of fast rotation, so that all the protons involved sample the same chemical microenvironment, like the three protons of a methyl group. Then the shorter distances will be weighted more in the peak intensity than the longer ones. This effect depends also on the mutual position of the atom or group and the methyl group giving rise to the crosspeak so that no prediction can be made a priori. Since all these intensities were translated later in upper and lower bounds on the distances we are quite confident that these bounds were chosen large enough to contain all the possible errors. Once the NOE's files were compiled the distances were computed making use of a program which takes into account, to a certain extent, also spin diffusion. First the NOE's are sorted by their intensities, then first order distances are computed, using the already calculated distances to describe the alternative relaxation pathways. Since the relaxation matrix contains the rotational correlation time and a scaling factor

(used to compute the absolute intensity of the NOE's from the experimental values) these were entered by trial and error until a satisfactory result was obtained for the fixed distances in the amino acids. Three complete sets of distances were then computed. Since not all the NOE's were present in the three spectra and the results were not always really the same an average was extracted weighting more the outputs for the shorter mixing times (in practice reasonable weights of 4, 2 and 1 respectively for 150, 300 and 600 msec. mixing times were used), and then upper and lower bounds on the interproton distances were compiled comparing these three sets of distances. We set the bounds up to $\pm 10\%$ of the computed distance when the variation of the data was within this range. When an NOE, not completely accounted for by spin diffusion, was present only on the longer mixing times spectra we set the lower bound on the distance to be in any case greater than 4 Å. In all other cases lower and upper bounds were chosen in order to contain all the three values obtained for the distance. Unfortunately not all the information we had got could be used since no stereospecific assignment had yet been made. So we had to relate all the bounds for these protons to "pseudo atoms" following the procedure described by Wüthrich et al. (1983). These "pseudo atoms" are taking over the average position average steric hindrance of the real atoms they are replacing. This was dictated by the choice to use the program DISMAN to obtain the 3D structure of the protein from the experimental bounds on the distances. This program makes use of these pseudo–atoms to handle the lack of stereospecific assignments. In this procedure information was obviously lost, as we will see, and the bounds on the pseudo atoms were chosen in order not to introduce any error.

STRUCTURE OF NISIN FROM DISTANCE CONSTRAINTS

The program DISMAN has been described in great detail (Braun & Gō 1983); it combines a fast algorithm for the minimization of an error function (a weighted sum of the squares of the experimental and the Van Der Waals radii bounds violations) and prior knowledge about amino acids geometry, so that the minimization is performed in the space of torsion angles rather than in the 3N–D space of the coordinates of the atoms. This greatly reduces the amount of time the program takes to produce a structure from the data. Unfortunately

the residue library of this program doesn't contain the unusual amino acids of Nisin so that, at least in the preliminary runs we have used a model peptide where the D–amino acids were obtained simply reversing the sign of one axis in the residue library in the coordinates and rotation vectors of the corresponding L–amino acids. So the Methyllanthionines and the Lanthionine were modelled by two Cysteines with a disulphur bridge requiring in addition the two sulphur atoms to be coincident weighting this requirement three times more than the other bounds (the corresponding Van der Waals energy term was removed from the error function specifying one of the two sulphur as pseudo–atoms). The dehydrobutyrine was simulated by a threonine with the OH group replaced by a pseudo–atom and Dehydroalanines were substituted with alanines. While we don't expect to introduce a big error in the replacement of Dha , Dhb and Lan, both sterically and geometrically, the simultaneous absence of the steric hindrance of a sulphur atom and a methyl group in the model methyllanthionine could greatly enlarge the conformational space of this residue. On the other hand the same replacement can help the conformation to come out of local minima (or completely remove these minima) during the run of the program through paths otherwise sterically forbidden in the energy map. This point was checked afterwards running the program using as starting structures the 10 best ones from the previous runs and using an updated residue library with the methyl group added. Although these were much sensible to initial conditions (in particular for what concerns the rings) 5 structures still with no major violations were obtained (the other 5 possessing local violations) and the backbone torsion angles were very close to the input values so that we are confident that the features discussed hereafter are still holding.In the following an analysis of the 15 preliminary runs is given and, when possible, a comparison is made with results obtained in other laboratories, both on the basis of the observed NOE's and of the structures produced by the program. We have considered well defined a dihedral angle when 8 of the 15 values were within a range of 60 degrees. The analysis was performed jointly on the angles file and the violations file so that structures with severe violations of the bounds were discarded (no violations of the Van der Waals constraints were found).

Residues 1–7) The first 7 residues comprising the first ring are expected to be well constrained judging by the amount of NOE's present. Most of the amide

to amide distances were found in a shorter range than the corresponding ones for water. Furthermore NOE's were found also among non adjacent residues (in addition to the obvious 3 to 7 crosspeaks), so that a rather compact structure is predicted. We can compare this with what found in the preliminary DISMAN runs, keeping in mind that there are some differences in the actual and the computed structures, and with what was reported by other authors (Palmer et al. 1989) who studied in great detail two model compounds for the ring 3–7 of Nisin by means of N.M.R. and subsequent energy minimization. As already noted some information is lost in the replacement of Dhb and Dha with Thr and Ala and also in the replacement of real atoms with pseudo–atoms so that despite the NOE's between the beta– of Dha_5 and the amide–protons the ψ angle of Dha_5 and the ϕ angle of Leu_6 were only broadly determined and probably the same can be stated for the psi angle of Dhb_2, here the main problem being connected with the uncorrect geometry. All the other backbone torsion angles tend to cluster around well defined values. Before making any comparison between the structures obtained in the present work and those obtained in the cited paper it is interesting just to compare the sets of NOE's. As long as a comparison is possible our data match completely the ones for the D–Ala ring A model compound for what concerns the first three residues while the sequential NOE's from 5 to 7 are different for both the model rings. What was found in the energy minimization of the D–Ala ring A was a Hydrogen bond between the acetic group attached to Alas and the amide proton of Ile. (The corresponding atoms are in our case the amide proton of ILe_4 and the carbonylic oxygen of Dhb_2). The formation of a hydrogen bond involving this proton could be in agreement with the observation of a large shift in its resonance frequency passing from water to water/TFE mixture. We checked the distance between these atoms on the structures which didn't present violations of the experimental constraints and this resulted always (with only one exception out of nine selected structures) in the range 2.8–3.2 Å. A representative picture of the first 7 residues is given in fig. 19.

Residues 8–11) Although the amount of NOE's was much lower than that found in water the NOE's derived distance constraints were similar so that no major changes are expected. For this ring a very detailed molecular study was also performed by Palmer et al. (1990) so that we can compare our results with

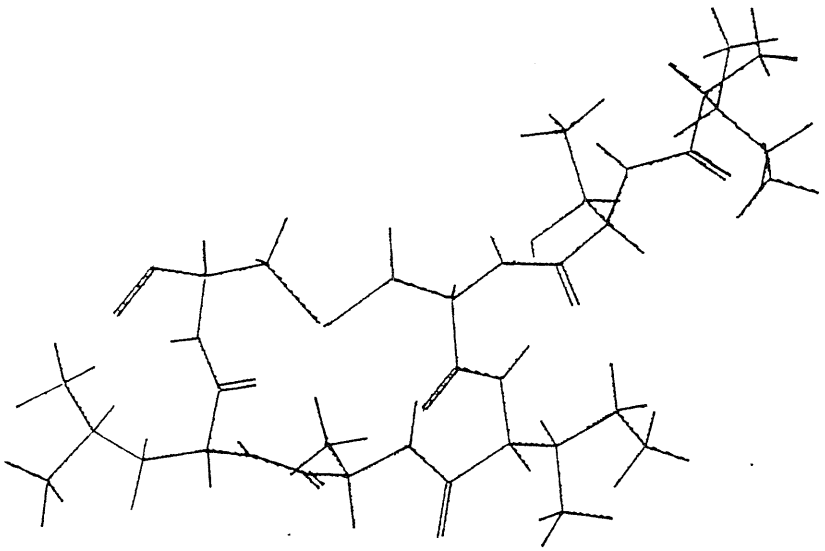

Fig. 19 Representative picture of residues 1–7.

theirs. One of the main features of this ring is the presence of a transannular hydrogen bond between between the carbonylic oxygen of $Alas_{11}$ and the amide proton of $Abas_8$. This seems rather feasible also in our case. In all the structures with no violations these two atoms were close in space (ca. 3Å) and it seems reasonable that this happens if steric hindrance inside the ring is to be avoided. This can be seen clearly in fig. 20.

In comparison with what was reported for Nisin in water (Slijper et al. 1989) we miss all the NOE's connecting this ring with residues 15,16 and 17; however it is not clear at this point if this reflects a real difference between the molecules in the two solvents or just the lower sensitivity of our experiments.

Residues 12–23) The preliminary DISMAN runs indicate that the bounds we have on the interatomic distances (at least in the simplified form involving the quasi atoms) are not sufficient to constrain this domain of the molecule. Also for this stretch of residues the amount of long range NOE's was lower than that found in water although some important crosspeaks were still present. For instance Ala_{15} is clearly seen to be faced with Asn_{20} and this should pose some limitations on the

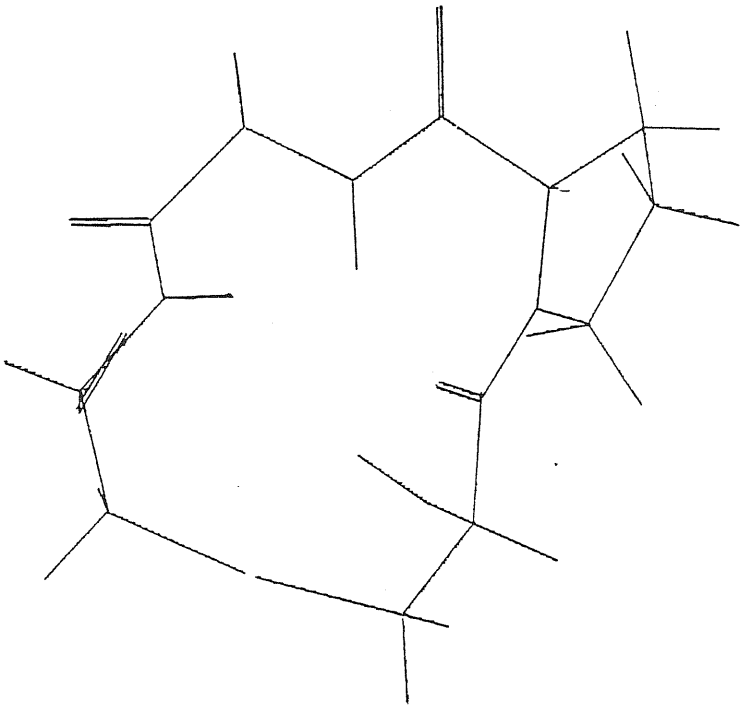

Fig. 20 Representative picture of residues 8–11.

conformational freedom of ring 13–19. However an analysis of this ring is not really straightforward since, notwithstanding these long range NOE's, several different structures could still satisfy all the constraints and it is difficult to say if this feature is just the outcome of not high enough sensitivity, lacking of stereospecific assignment, both of these or real conformational freedom. An important feature is the presence of a II–type beta turn at residue 22–23 and the corresponding backbone torsion angles were found to be well constrained in the corresponding region of the Ramachandran plot (Wüthrich 1986). This feature was already suggested by Chan et al. (1989) on the basis of the experimental NOE's found in water.

Residues 23–34) This stretch comprises the entangled double ring system. Due to the two monosulphur bridges limiting the conformational freedom we expect residues 23 to 28 to be well constrained. Indeed the backbone torsion angles are found around well defined values in the DISMAN runs. Also for these two rings the formation of transannular hydrogen bonds is quite feasible. In the structure shown in fig. 21, for instance, the distances between the carbonylic oxygen of $Abas_{23}$ and

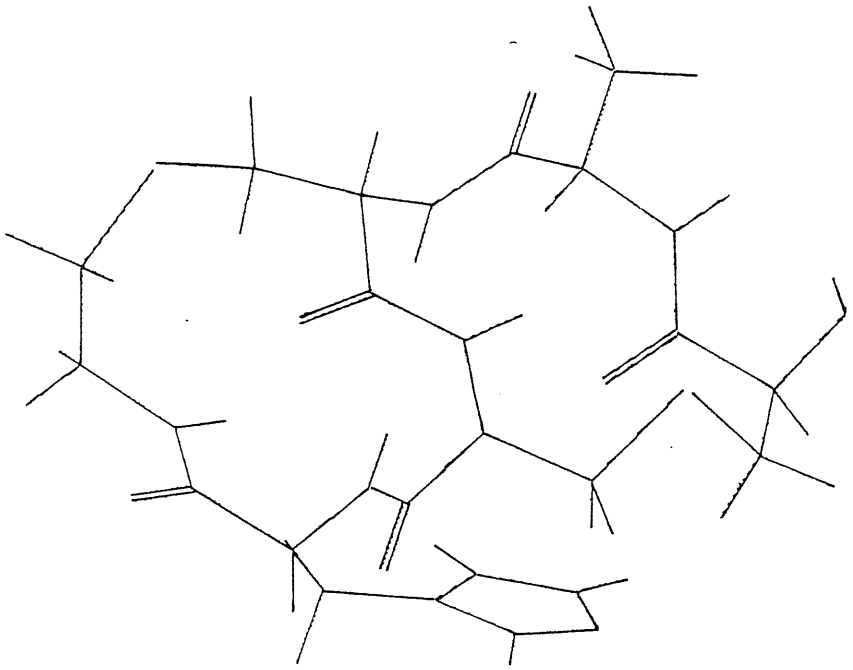

Fig. 21 Representative picture of residues 23–28.

Abas$_{25}$and the amide protons of Alas$_{26}$ and Alas$_{28}$ are 3.0Åand 1.8Årespectively. In all the structures with no violations the distance between the two atoms in the first ring was in the range 1.8–3.0 Åwhile the second ring was not so well constrained neverthless very low values (1.8Å) were still found. What was more surprising was to find also the final part of the molecule in a rather well defined conformation despite what found in water by other researchers. A representative picture of this stretch of the molecule is given in fig. 22.

For aqueous environment very weak or missing inter–residual NOE's were reported for residues 29–34 leading to the conclusion that this stretch of residues is in a rather flexible conformation. On the contrary we found a continuous walk of NOE's (all the alpha to amide protons crosspeaks from residues 28 to 31) some of which were quite strong. The presence of a sudden turn at residues 30–31 was apparent in several structures.

CONCLUSIONS

Resuming the discussion so far we can stress two points of interest:

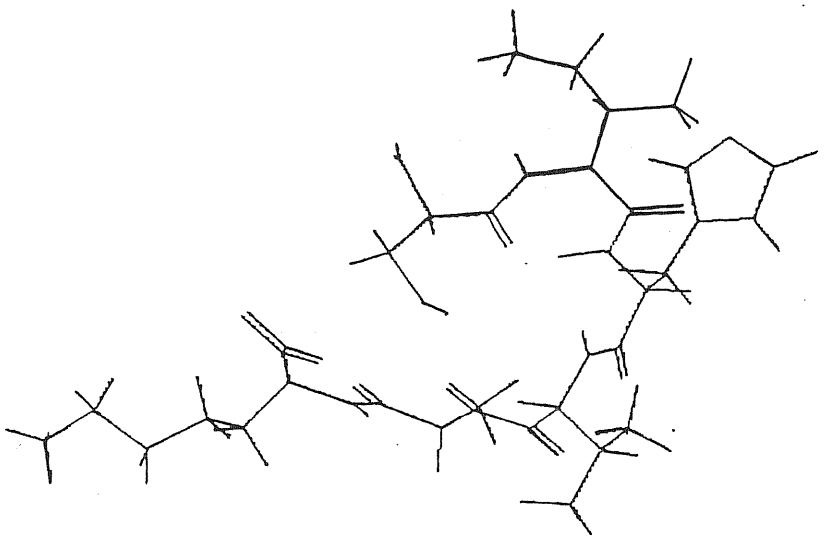

Fig. 22 Representative picture of residues 29–34.

1) the differences in the present results compared to the analogous ones obtained in water (Slijper et al. (1989)) are mostly concerning the final part of the molecule and the missing long range NOE's although this is a rather subtle point. These differences are however not enough to suggest anything about how Nisin is acting on lipid membranes. A better defined answer to this question could probably come from experiments in SDS.

2) The possibility of hydrogen bonding in the methyl–lanthionine rings (this was found in all the three rings composed by only four residues) could be an efficient way to stabilize both geometrically and energetically these structures, while, at the same time this could suggest more conformational freedom in the other (larger) rings where such feature is not observed. Further steps are required to establish on a more solid ground these suggestions. Namely to run the same program making fully use of the stereospecific NOE's derived constraints, and using an updated residue library containing all the unusual amino acids of Nisin. Then energy minimization and molecular dynamics could give a better picture of the molecule. Work is being done in this direction.

References

Abragam A., Principles of Nuclear Magnetism (1961), Oxford University Press, London.

Altona C., Recl. Trav. Chim. Pays Bas (1982) **101**, 413–433.

Aue W. P., Bartoldi E. & Ernst R. R., J. Chem. Phys. (1975) **64**, 2229–2246.

Bain A. D., J. Magn. Res. (1984), **56** , 418–427.

Bax A. & Davis G., J. Magn. Res. (1985) **65** , 355–360.

Bodenhusen G., Kogler H. & Ernst R. R., J. Magn. Res. (1983), **58**, 370–388.

Bodenhausen G., Vold R. L. & Vold R. R., J. Magn. Res. (1980) **37**, 93–106.

Bothner–By A. A., Stephens R. L., Lee J.–M., Warren C. D. & Jeanloz R. W., J. Am. Chem. Soc. (1984) **106**, 811-813.

Braun W. & Gō N., J. Mol. Biol. (1985) **186**, 611–626.

Braunschweiler L. & Ernst R. R., J. Magn. Res. (1983) **53**, 521–528.

Buchman G. W., Banerjee S. & Hansen J. N., J. Biol. Chem. (1988) **263**, 16260–16266.

Cavanagh J., Chazin W. J. & Rance M., J. Magn. Res. (1990) **87**, 110–131.

Chan W. C., Lian L.–Y., Bycroft B. W. & Roberts G. C. K., J. Chem. Soc. Perkin Trans. (1989) **12**, 2359–2379.

Engelman D. M., Steitz T. A. & Goldman A.,Ann. Rev. Biophys. Chem. (1986) **15**, 321–353.

Ernst R. R., Bodenhausen G. & Wokaun A., Principles of Nuclear Magnetic Resonance in one and two dimensions (1989), Oxford University Press, Oxford.

Fano U., Rev. Mod. Phys. (1957) **29**, 74–93.

Griesinger C., Otting G., Wüthrich K. & Ernst R. R., J. Am. Chem. Soc. (1988) **110**, 7870–7872.

Gross E. & Morell L., J. Am. Chem. Soc. (1971) **93**, 4634–4635.

Heberlen U. & Waugh J. S., Phys. Rev. (1968) **175**, 453–467.

Henning S., Metz R. & Hammes W. P., Int. J. Food Microbiol. (1986) **3**, 121–134.

Hurst A., Adv. Appl. Microbiol. (1981) **27**, 85–123.

Ingram L., Biochim. Biophys. Acta (1970) **224**, 263–265.

Levitt M. H., Freeman R. & Frenkiel T., Adv. Magn. Res. (1983) **11**, 47–110.

Kaletta C. & K–D Entian, J. Bacteriol. (1989) **171**, 1597–1601.

Knox J. R. & Keck P. C., Biochem. Biophys. Res. Com. (1973) **53**, 567–571.

Knox J. R. & Keck P. C., Acta Crystallogr. Sect. B (1975) **31**, 2698–2700.

Kordel M. & Sahl H.–G., FEMS Microbiol. Lett. (1986) **34** 139–144.

Kühlbrandt W., Q. Rev. Biophys. (1988) **21**, 429–477.

Macura S. & Ernst R. R., Mol. Phys. (1980) **41**, 95–117.

Morris A. G. & Freeman R., J. Magn. Res. (1978), **29**, 433–462.

Morris S. L., Walsh R. C. & Hansen J. N., J. Biol. Chem. (1984) **259**, 13590–13594.

Palmer D. E., Mierke D. F., Pattaroni C., Goodman M., Wakamiya T., Fukase K., Kitazawa M., Fujita M. & Shiba T., Biopolymers (1989) **28** 397–408.

Rance M., Sørensen O. W., Bodenhausen G., Wagner G., Ernst R.R. & Wüthrich K., Biochem. Biophys. Res. Com. (1983) **117**, 479–485.

Reisinger P., Seidel H., Tschesche H. & Hammes W. P., Arch. Microbiol. (1980) **127**, 187–193.

Ruhr E. & Sahl H.–G., Antimicrob. Agents Chemoter. (1985) **27**, 841–845.

Sahl H.–G., Kordel M. & Benz R., Arch. microbiol. (1987) **149**, 120–124.

Schnell N., K.–D. Entian, Schneider U., Götz F., Zähner H., Kellner R. & Jung G., Nature (1988) **333**, 276–278.

Solomon I., Phys. Rev. (1955) **99**, 559–565.

Slijper M., Hilbers C. W., Könings R. N. H. & Van de Ven F. J. M., FEBS Lett. (1989) **252**, 22–28.

Vega S., , J. Chem. Phys. (1978) **68**, 5518–5527.

Van de Ven F. J. M. & Hilbers C. W., J. Magn. Res (1983) **54** ,512–520.

Wokaun A. & Ernst R. R.,, J. Chem. Phys. (1977)**67**, 1752–1758.

Wagner G., Pardi A. & Wüthrich K., J. Am. Chem. Soc. (1983) **105**, 5948–5949.

Wüthrich K., Billeter M. & Braun W., J. Mol. Biol. (1983) **169**, 949–961.

Wüthrich K., N.M.R. of proteins and nucleic acids (1987), John Wiley & Sons, New York.

Acknowledgements

I wish to thank prof. Borsellino who supported this work, prof. Hilbers who accepted me in his laboratory and organized my staying there, Frank Van de Ven who taught me almost everything I know on 2D–NMR. I wish to thank Babs de Klink, Nelly Kersten–Piepenbrok and John Roef for all the help I received from them. Jos Jordaens is gratefully acknowledged for patient and expert help in the Computer Kamer. I took also profit of discussions with the "young bright scientists" populating the underground of the biophysical chemistry department namely Paul Folkers, Margaret Mooren, John van Duynhoven, Henno van de Hooven, Rob Schouten. Moreover I want to thank all the people at the University of Nijmegen who made my staying in Holland a really good time. I wish also to thank Gilberto Giugliarelli for patient and expert help with the computer and Franca Aicardi for all the help during these two years at S.I.S.S.A.. This work was financially supported by Fondazione Angelo Della Riccia.